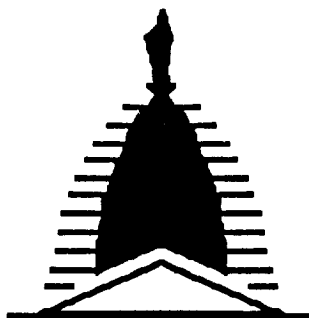


1.1



**UNIVERSITY of
NOTRE DAME**

**NASA/USRA UNIVERSITY
ADVANCED DESIGN PROGRAM
1989-1990**

**UNIVERSITY SPONSOR
BOEING COMMERCIAL AIRPLANE COMPANY**

FINAL DESIGN PROPOSAL

THE STEALTH BIPLANE

**A Proposal in Response to a Low Reynolds Number
Station Keeping Mission**

May 1990

**Department of Aerospace and Mechanical Engineering
University of Notre Dame
Notre Dame, IN 46556**

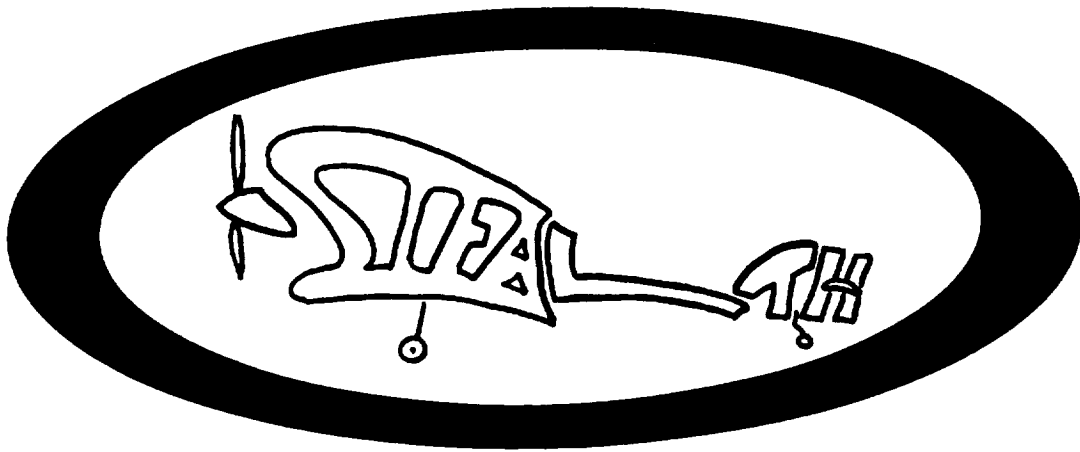
(NASA-CR-186680) THE STEALTH BIPLANE: A
PROPOSAL IN RESPONSE TO A LOW REYNOLDS
NUMBER STATION KEEPING MISSION Final Design
Proposal (Notre Dame Univ.) 100 p CSCL 01C

N90-25127

Unclass

G3/05 0289179

Design Group "B" Presents:



The "Stealth Biplane"

Chief Design timothy e. walsh

Propulsion Team: kevin t. flynn
 steven donovan

Aerodynamics Team: chris paul
 timothy e. walsh

Structures/Materials harold pangillinan
 john padgett

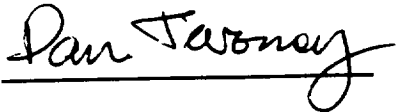
Stability & Controls daniel twomey



Timothy E. Walsh



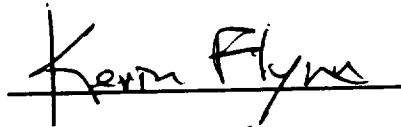
Steven Donovan



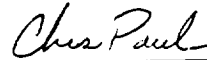
Daniel Twomey



Harold Pangilinan



Kevin T. Flynn



Chris Paul



John Padgett

Executive Summary

The Stealth Biplane is conceived and constructed to serve as a remotely piloted vehicle designed to navigate a low-level figure-eight course at a target Reynolds number of 100,000. This flight vehicle will combine the latest in lightweight radio controlled hardware in conjunction with current low Reynolds number aerodynamic research to demonstrate feasible operation in a variety of applications. These potential low Reynolds number applications include high altitude atmospheric sampling, search and rescue, and even law enforcement.

The completed prototype is designed to operate within the Loftus Indoor Athletic Facility at the University of Notre Dame. The course and flight plan within this facility are displayed in a drawing at the end of this executive summary. Briefly, this course requires an unassisted ground takeoff followed by a climb to cruise altitude of 20 feet, in position to make the first left hand turn. Upon completion of the turn, a slight loss of altitude is predicted; however, the ensuing straight cruise portion of the flight affords this lost altitude to be regained. A similar right hand turn and subsequent straight cruise complete one full lap around the course. Upon the completion of three full laps around the course, the Stealth Biplane will need to loiter back to the opposite end of the field for the landing run, where a full stop ground landing will then be executed. This flight plan fulfills all imposed design requirements for normal operation.

Safe operation around such a course can be accomplished by an experienced ground based pilot, but the pilot workload should be sufficiently light such that even an amateur can control the Stealth Biplane. In order to

successfully rotate the Stealth Biplane and ascend to the mission altitude of 20 feet, a powerful propulsion system is required.

The electric motor that was selected to fulfill all of the mission requirements was the Peck Silver Streak 035M electric motor, capable of producing a maximum static thrust of 11 Newtons and a maximum power of 95 watts. At this power setting, the engine operates at 13,000 rpm and uses an 8 inch diameter, 4 inch pitch *Rev - Up* propeller. This propulsion system derives its power from a power pack of 10 AA Nickel-Cadmium 1.2 Volt, 600 mAh rechargeable batteries. This entire powerplant will allow the aircraft achieve its required cruising velocity of 28 ft/s, with a maximum velocity of 40 ft/s. This propulsion system was selected for its relatively low weight of only 10.6 ounces, lowering the total aircraft weight significantly. The most important factor in selecting the aircraft propulsion system was obtaining the necessary power required for take-off. The Peck Silver Streak electric motor will provide sufficient power to successfully allow the Stealth Biplane to complete the mission.

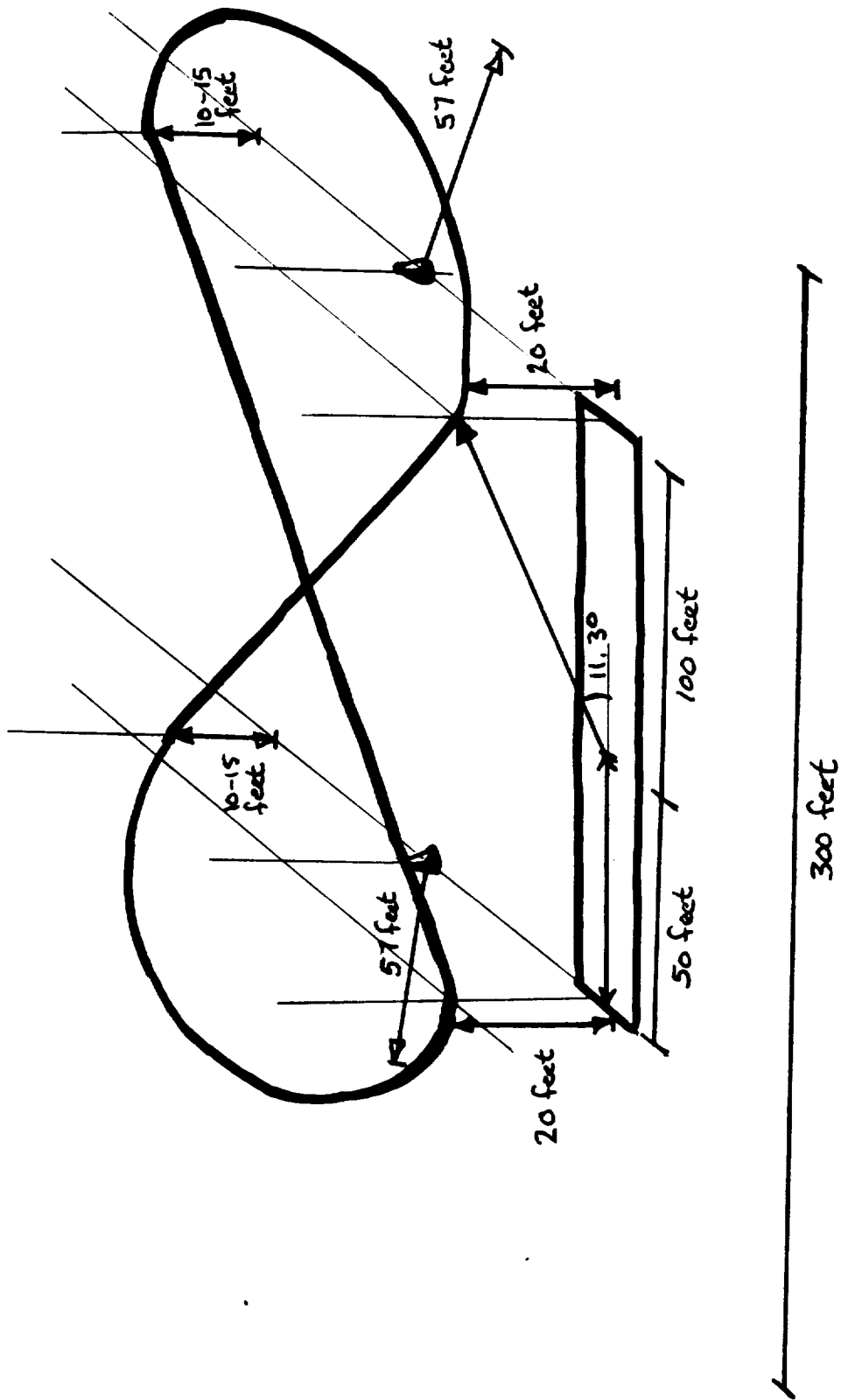
The Stealth Biplane will be receiving its lift from twin lifting surfaces in the form of a staggered biplane wing configuration. The top or main wing measures 4 feet in span, with a root chord length of 8 inches, a taper ratio of 0.65, and a mean chord length of 6.6 inches. The lower, staggered wing measures 3 feet in span, with the same root chord, taper ratio and mean chord length as the top wing. The lower wing is staggered 3.2 inches aft and 9 inches below the leading edge of the main wing. Neither surface is swept; thus, the surface areas of the wings measure 2.2 ft² and 1.65 ft² for the top and bottom wings respectively. The airfoil selected for both surfaces is the Wortmann FX 63-137 airfoil. However, the lower wing has been

augmented with a 5 degree droop of 13 % of the chord at the leading edge, for an overall increase in L/D for that surface.

The construction of the Stealth Biplane requires a variety of fabrication techniques; the wing ribs, spars, and stringers will be fabricated from balsa, and the wing skin will be a mylar-based derivative like Monokote™. The fuselage is constructed from four 2 inch x 14 inch balsa sheets in a boxlike configuration, with the propeller in the front of the aircraft and the components strategically placed to ensure static and dynamic stability of the Stealth Biplane. The empennage is a simple 1.5 inch diameter balsa cylinder which will connect the horizontal and vertical tails with the main fuselage. This cylinder has been designed to provide optimum tail control while still minimizing the overall weight of the aircraft. The empennage (movable rudder and elevator) is constructed from simple flat plates of solid balsa, and the components are controlled by two Futaba RG 141T microservos.

Some topics that will require further discussion as the Stealth Biplane transitions from ideas and sketches to an invincible remotely piloted vehicle capable of fulfilling all of the mission requirements include: maximum deflection distance of the empennage control systems, ground effect influence on take-off performance, and yaw corrections for the lack of ailerons.

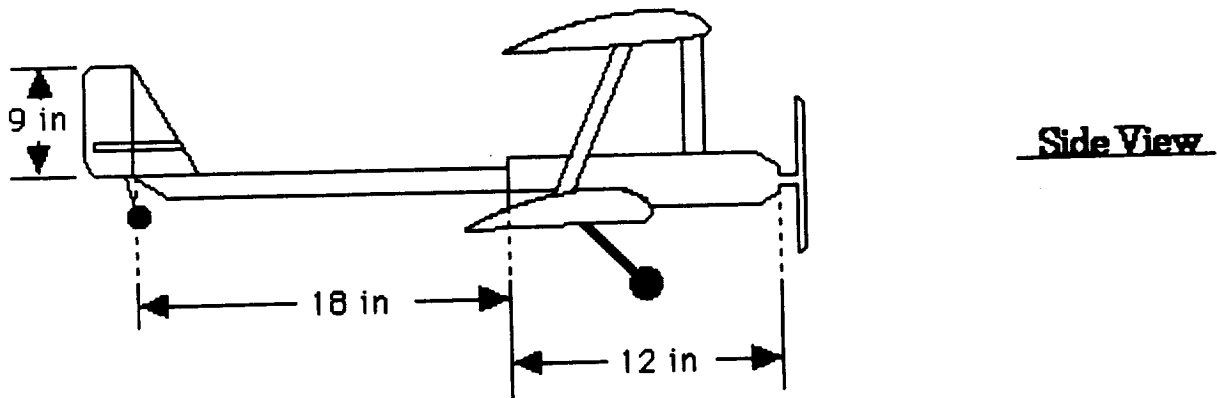
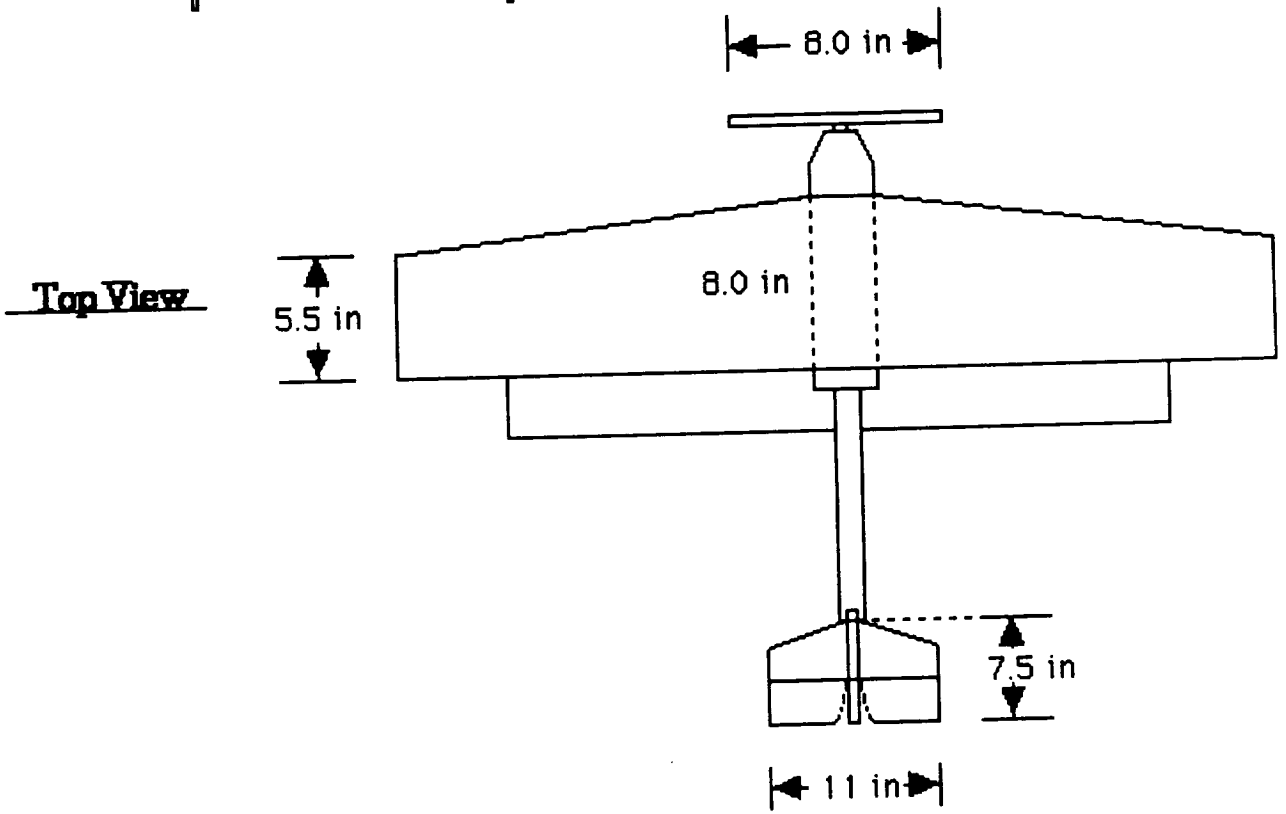
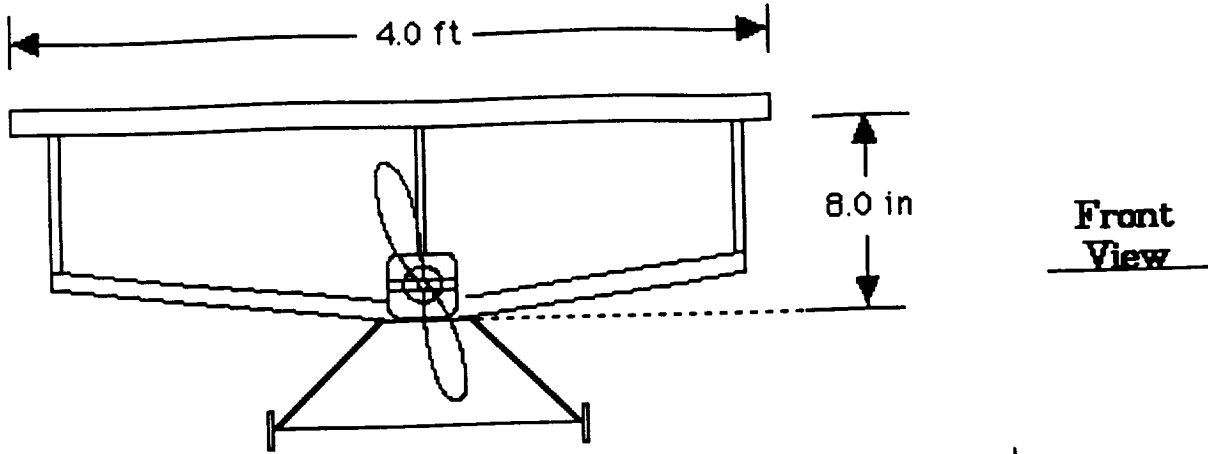
Discussion of the final Stealth Biplane prototype has been very important over the last 9 weeks of this design course, and we are confident that our aircraft will safely complete all of the mission and design requirements, and travel on to top performance at the USRA conference.



Misson Course

GROUP "B"

THE SNEALTHI BIPLANE



Specification Summary

specification	range	symbol
Endurance	4 min 15 sec @ full throttle	E
Motor Type	Peck Silver Streak 035M	
Motor Power	95 W @ 13,000 rpm	P
Fuselage Dimensions	2" x 2" x 14"	
Takeoff Distance	37 feet	S_{to}
Landing Distance	50 feet	S_{td}
Max. Load Factor	1.5	n
Aircraft Weight	41.6 oz	W
Propeller Type	Rev-Up 8-4 (2 bladed)	
Range	+ 3000 ft	R
Reynolds Number	98,000	Re
Speed	22 - 40 ft/s	$V_{stall} - V_{max}$
Wing Dimensions		
Surface Area	2.2 ft ² (top) 1.65 ft ² (bottom)	S_{top} S_{bottom}
Root Chord	8.0 inches	c_{root}
Mean Chord	6.6 inches	c_{mean}
Taper Ratio	0.65	λ
Span	4.0 feet (top) 3.0 feet (bottom)	b_{top} b_{bottom}
Aspect Ratio	7.273 (top) 5.455 (bottom)	AR_{top} AR_{bottom}
Dihedral	2° (top) 10° (bottom)	ϕ_{top} ϕ_{bottom}
Angle of Incidence	2° (top) 6° (bottom)	$\alpha_{i\ top}$ $\alpha_{i\ bottom}$
Vertical Tail Area	54 in ²	$S_{v\ tail}$
Horizontal Tail Area	99 in ²	$S_{h\ tail}$

Mission Statement

The assignment distributed at the beginning of this course required the design and eventual fabrication a remotely piloted vehicle that is to perform as a pylon racer. The course to be flown consists of two pylons placed 50 yards apart. The aircraft must successfully take off, complete three laps of the designated figure eight course and then come to a safe landing. At no time during this flight may the altitude exceed 25 feet nor the flight Reynolds number exceed 200,000. Consequently, the aircraft will be flying at very low flight speeds. In addition, the design restrictions require the ability to disassemble the aircraft and store it in a 2'x2'x4' container and then reassemble it in under half an hour. Also, the propulsion system must be non-airbreathing and must not emit mass. Each of these restrictions must be kept in mind during the design, construction, and flight phases of this assignment.

As mentioned in the handout, this mission is meant to simulate the flight of a sailplane. Such an aircraft is required to fly at very low speeds at both high and low altitudes. This study will help us get a better understanding of the difficulties associated with such flight. For instance, it was discovered that drag can be very high at these low speeds. At such low Reynolds numbers several types of boundary layer behavior may occur. In one case, laminar separation occurs near the leading edge causing the aircraft to stall. Another possibility is that a separation bubble could occur and drastically decrease the efficiency of the airfoil. Finally, the preferred case occurs when the flow is laminar up to the adverse pressure gradient when it turns turbulent and retains enough power to remain attached. This case is associated with the least drag. In addition, a study shall be

conducted on the effect that these low velocities have on the aircraft's maneuverability. It should be noted that because of the sensitivity of the low Reynolds number airfoil boundary layer to freestream and surface generated disturbances, definitive experiments are very difficult to achieve.

From the mission statement the aircraft's voyage can be separated into three critical stages: 1) takeoff, 2) turning, and finally 3) landing. For this first stage the RPV must be able to achieve takeoff velocity within the designated runway. To assist in this goal, airfoil and engine selection play an important role. The airfoil must be very efficient and reasonable to construct. The engine must provide sufficient thrust and be light weight. The landing gear will also play an important role in achieving successful takeoff since it is beneficial to reduce the friction drag between the wheels and the astroturf.

For negotiating the turns, the control surfaces will play a major role in the success of our mission. We believe that a good rule for control will be the larger the control surface the better. To better understand the types of turns the aircraft will be negotiating, the course was approximated as two semi-circles about the pylons. This served as a rough estimate of the total course length which were found to be about 2,250 ft. This also helped to get a better power required estimate because the majority of this flight will be spent in a banked turn. Such flight will require more power than that demanded in steady level flight.

From the maximum allowed Reynolds number of 200,000, a target Reynolds number of 100,000 was decided upon. With this goal in mind it is possible to determine the cruise velocity as a function of mean chord length. The maximum velocity will be dictated by a minimum chord length while the minimum velocity will be given by the aircraft's stall characteristics. For

subsequent calculations the values for cruise velocity and chord were approximated to be 30 ft/s and 6 in., respectively. With these estimates in mind the time of flight can be approximated to be 2-3 minutes. These estimates should assist in selecting a power source to meet the needs of the mission.

The final segment of the mission will be the landing portion. The most important factor for success in this area will be sturdy landing gear. This is true because the use of good landing gear will take care of a major concern in this assignment which is safety. What will play an important role in this portion of the mission as well as the others will be speed control. Through speed control it is possible to achieve the most efficient use of our power source by providing the most power at critical times like takeoff and turns and then reducing the power and, thus, velocity to ensure a safe landing.

By keeping both the mission requirements and the design objectives in mind and using sound engineering judgement, Group B hopes to successfully complete the stated task.

Concept Selection Studies

One of the first steps taken after the mission was assigned was for each member of the design group to propose his own concept of what the aircraft should look like in order for it to successfully complete this mission. At the time we had only a basic idea of what this aircraft should look like. These initial ideas were based on the mission constraints provided. For instance, due to the low Reynolds number requirement it was known that this aircraft would have to maintain flight at very low speeds. Consequently, it was understood that this aircraft would require a large amount of lifting surface. Other objectives included:

1. **Size** - the aircraft must be capable of being taken apart and stored in a 2' by 2' by 4' container. Assembly must take no longer than a half hour.
2. **Weight** - by maintaining a minimum weight we can reduce our material costs as well as the cost and weight of the propulsion system, thus reducing our power requirements.
3. **Cost** - we have a budget of \$180 for this project. Every effort must be made to reduce production costs and keep the project within budget.
4. **Maneuverability/Controllability** - this aircraft must be capable of negotiating the designated figure eight flight path.
5. **Safety** - we must fly this aircraft within the Loftus Athletic Facility with minimal damage to the aircraft, ourselves, and the facility.
6. **Takeoff and Landing Distance** - a mission constraint is a maximum 50 yard runway.

Keeping both the mission requirements and the design team's objectives in mind the group produced several basic concepts for the aircraft design. There was support for a standard, high aspect ratio

monoplane, a monoplane or biplane with a twin boom fuselage structure, and overwhelming support for a biplane. Despite the overwhelming support for the biplane the design team felt that it would be worthwhile discussing the advantages and disadvantages of each of these aircraft.

First, the proposal for a standard monoplane with high aspect ratio was discussed. There were several advantages to such a design. There already exists a large data base which could be used to assist in both the design and construction stages. Another advantage of such a design is the past experience that some of the design team members have had with constructing and flying similar aircraft. In addition, we also discussed concept selection with several members of last year's class and found that there was overwhelming support for a monoplane design - the monoplane has simpler aerodynamics, less induced and interference drag, and more stability. The only uncertainties were with controllability in the enclosed arena, structural strength of a monoplane wing, and any difficulties that might occur at such low flight speeds.

The second concept considered was similar to the first with the exception of the fuselage which would have been a twin boom configuration. A similar design was chosen last year because of the benefits a twin boom has from a stability and control standpoint. Because of the important role stability and control will play in this mission, serious consideration was given to this design and its advantages and disadvantages. It was hoped that the two booms would provide this stability and, in addition, be very lightweight and have little drag associated with them. Unfortunately, the structures team felt that for there to be any significant benefit in control and weight, we would face probable failure due to the torsion and bending loads

imposed on the booms during normal flight conditions. Consequently, this concept was dropped from further consideration.

Finally, the third design proposal considered was a basic biplane configuration. Unlike the standard monoplane, there is not a large amount of data available on remotely piloted biplanes. This is especially true for biplanes flying at low Reynolds numbers like the speeds required in this mission. It is a well known fact that in general there is more drag (parasite and induced) associated with a biplane than with standard aircraft. Still the design team felt that a biplane could successfully complete this mission.

The biplane is a small, sturdy aircraft that is very maneuverable. It has better stall qualities than standard aircraft and is capable of landing and taking off in shorter distances. The two wings provide the same amount of lifting surface as a standard airplane while taking up less spanwise space. In addition, the wings of the biplane are subject to smaller bending loads. Consequently, a lighter wing structure is possible. Another very important factor that may have tipped the scale in favor of the biplane was the group's overall curiosity. Because there will be a great deal of time and effort invested in this project the design team wanted it to be something that will hold its interest and that has not been attempted in years past. These characteristics, in addition to overall curiosity in a biplane, led us to begin studying the different possibilities that existed in biplane design.

Once the decision was made on a biplane configuration there were several other aspects of the aircraft that needed to be discussed. The design team discussed the value of performance enhancers like ailerons, wing sweep, dihedral, flaps, and wing planform. The first of these that was investigated was the use of ailerons. The advantage of ailerons is that they can help the aircraft maneuver around the pylons. Still, they require an

addition pair of push rods and a discontinuous wing. As previously mentioned such disturbances can cause undesirable behavior in the airfoil boundary layer. In addition, they add weight and create special construction problems. These undesirables can be avoided if sufficient wing dihedral is included in the design and the pilot uses both rudder and elevator controls to negotiate turns. Dihedral works with the vertical fin to maintain steady level flight by preventing roll. However, too much dihedral will cause the aircraft to Dutch roll. The dihedral also helps to translate the yaw produced by the rudder movement into a banked turn. It does this by taking the extra lift on the outside wings and using it to make the turn and at the same time helping stop the aircraft from slipping through the air.

Wing Concepts

We began our study of wing design by discussing the possibility of a biplane with two wings with a large degree of sweep. It was discovered that sweep is primarily used to eliminate shock waves that can occur over the top of a wing at high speeds. Because the wing only "sees" the velocity component normal to the wing, sweep enables a plane to fly at higher speeds and avoid undesirable shock waves. Such flight speeds are out of the regime that this aircraft will encounter. The design team felt it would be interesting to investigate what type of wing could best assist us in getting our aircraft airborne and around the pylon course. For example, it was discovered that delta wings have acceptable flight characteristics through most speed ranges. However, here the concern is very slow speed flight and the general rule of thumb is that the more wing span an aircraft has, the slower and more docile it will fly. Consequently, the team looked at both constant chord and tapered wings.

While a tapered wing is more difficult to construct it serves to distribute the loads on a wing in a near elliptical manner. We felt that such a tapered shape would leave us with a more desirable load distribution over the wing. In addition, such wings are very efficient and have less associated drag. Therefore, in this case, the team decided that despite the difficulties in construction it would be worth the effort to construct tapered wings in order to enhance performance. Still, there were other instances when it was decided that despite benefits to performance, the particular performance enhancer was not worth the time and money. For example, flat plates were chosen for our control surfaces as opposed to cambered airfoil. We also decided to construct the majority of the aircraft from balsa in order to ease construction. It is often the case where additional performance enhancers and more complex designs cause unnecessary headache and increase the possibility of failure. Consequently, we decided to keep the design as simple as possible given our current skills and resources.

Fuselage Concepts

In selecting a fuselage design the structures team attempted to keep drag and weight to a minimum as our primary design objectives. Still, there is a certain payload that the aircraft is required to carry. This payload includes the propulsion system, the servomotor, all associated electronics, and room for motor ventilation. It was discovered that a teardrop configuration would be associated with the least drag. Still, such a design is difficult to construct given the materials and tools provided. Consequently, a compromise was reached and the team decided on a fuselage whose forward section would be of a truss construction capable of housing the propulsion system and electronics. The rear portion of the fuselage is simply a balsa

cylinder, for its only function is to connect the forward fuselage section and wing structure to the tail. By combining these two sections the structures team tried to compromise and design a fuselage that meets both the design objectives and the mission requirements.

Propulsion Concepts

In choosing a propulsion system the propulsion team was limited to systems which are not airbreathing and do not emit mass. This leaves a choice of either a rubber band powered engine, an electric motor, or a CO₂ powered engine (which was considered not to emit mass). An electric motor was soon decided upon because of its availability and use in prior successful missions. From the beginning, there were doubts about the endurance and controllability of a rubber band powered engine. On the other hand, not enough information was available about the CO₂ engine. In retrospect, it is felt that the right decision was made because an extremely light weight engine has been found which provides ample power for our aircraft to complete its mission.

Tail Concepts

As stated before, both the single and twin boom were possible designs for our aircraft. Having chosen the single boom, the next step was to find an adequate tail structure. In choosing a tail we considered both a standard tail and a T-tail. The T-tail is displaced from the disrupted flow behind the fuselage and wing. It is not as affected by the downwash from the wing as a standard tail is, thus, reducing drag and maintaining effectiveness. Still, such a configuration would require a more difficult push rod arrangement

making controllability more difficult and, in addition, more subject to structural failure.

Summary

So here we have traced the development of our aircraft from our initial ideas and concepts to where it stands now. While in certain areas it may not be the best possible design, it is a compromise of ideas and the resources available. Attached is a diagram of this final concept. This design group believes that an electric powered biplane configuration is indeed feasible to construct, and further, the design group is confident that the final product is capable of completing this mission.

Aerodynamic Design

Wing Design

At the very outset of the design process, constraints on the design are imposed due to the nature of the mission. For our case, the first immediate constraint concerning the design of the wings is a maximum span length limitation. A strict ground handling constraint is the requirement that the entire aircraft be able to disassemble into a 2'x2'x4' packing box. It is desired that each of our wings be constructed in one continuous piece to increase the overall rigidity and eliminate the need for connecting and dismantling the wings. This requirement fixes the maximum span to four feet. Thus, the span for the top wing is set to four feet, while the span for the lower wing is set to three feet. The reason for this difference is that two wings each four feet in span would produce unnecessary weight additions to the aircraft as well as providing inefficient lift. A root chord of 8" was chosen on the basis of a desired flight velocity of 25-30 ft/s.

It is desirable to produce a wing planform resulting in a high lift to drag ratio, low drag, and lift with an elliptic distribution over the span for the least induced drag. With the span lengths known and zero wing sweep chosen to ease construction, the entire shape of both wings can be expressed by defining the taper ratio. The primary tool used in the investigation of certain parameters due to the variation of taper ratio is a software program called "Lin-Air" for the Apple Macintosh microcomputer. This software package approximates the lift over any wing planform by the use of the Vortex Lattice Method through horseshoe vortices and control points¹. In the Lin-Air program, half of the top wing was modeled using

¹ Dr. R. C. Nelson, Atmospheric Flight Mechanics, published by author, page 2.22.

eight control points and symmetry applied to find the total aerodynamic forces on the wing. The bottom half was modeled using only six control points. This was done such that the control points of the top and bottom wings would line up horizontally and not interfere with each other. It is believed that this number of control points will give sufficient accuracy in results considering the other assumptions made in this theory, such as modeling the wing as a flat plate.

After entering preliminary information concerning the general shape and location of the flat plate modeled wings into Lin-Air such as area, span, cruise velocity, dihedral, incidence, gap, and stagger; the taper ratio is simply altered as a basic input. The results (spanwise lift distributions, total lift and drag coefficients for both wings, and moment coefficients) then may be plotted in any way desired.

Below are figures (figure 1) showing the effects of taper ratio on lift, lift to drag ratio, and lift distribution. The figures indicate that the design should avoid very low taper ratios due to wing tip stall and very large taper ratios due to dramatic losses in (L/D). By varying this parameter, a taper ratio of 0.65 is found to have the best compromise in performance. It results in a decent (L/D) value while still maintaining a respectable efficiency, and a good semi-elliptical lift distribution while avoiding premature tip stall.

Both wings will be constructed with a rib and spar structure, a method common to small RPV's of this size and weight. By using balsa wood as the primary construction material, a very lightweight yet strong structure can be built with a minimum amount of time and effort. The choice of materials for the wing, fuselage, and empennage are covered more fully under Material Selection. In addition, an aerodynamic skin to cover the wing structure is

required. Coverings vary in breaking strength, impact strength, and tear resistance, but the Super MonoKote™ brand film covering seems to provide the best overall skin.

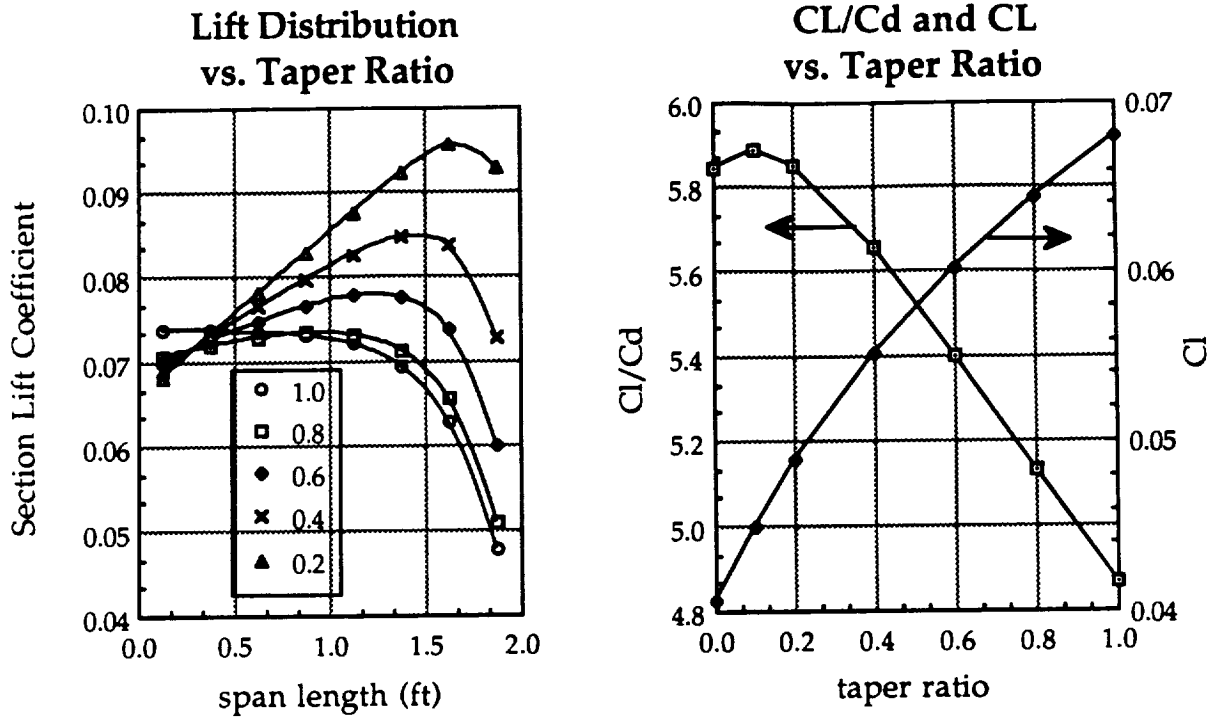


Figure 1

Airfoil Selection

In selecting an airfoil for the Stealth Biplane it is important to understand the requirements made on the aircraft due to its mission. First, the flight condition is the "low Reynolds number" flight regime which requires the use of an airfoil specifically designed for low Reynolds numbers and low speeds. Second, since the wing, and more specifically, the spars must serve as beams carrying the design load, the thickness of the airfoil

must be sufficient at the places where the spars must be located in order to carry these loads.

Several parameters taken together suggested the Wortmann FX 63-137 to be the most suitable airfoil for this mission. The Wortmann airfoil compares favorably when considering its high lift coefficient, good lift to drag ratio, relatively high stall angle, and sufficient thickness. In addition to these figures of merit are some additional considerations that influenced the final airfoil decision. First is structural considerations. The depth of a section determines the maximum depth of the wing spars; and the enclosed cross-sectional area is a measure of its ability to resist torque created by the pitching moment. Also, spar weight is inversely proportional to the square of the beam depth². Therefore, the deeper the spar and the thicker a section, the lighter the required wing structure. Second, since stall speeds and stall qualities lie at the heart of airworthy flying qualities, attention must be paid to the shape of the Wortmann's lift curve at the point of stall. The gradual peak indicates its docile stall characteristics. Lastly, ease of manufacture is adequate for the Wortmann. Since inexperienced craftsmen will be cutting small, fragile ribs, the shape and manufacture of the rib must be considered.

Figure 2 below shows the infinite lift and drag coefficients for the Wortmann airfoil on the left and, as a comparison, lift and drag coefficients for the finite wing configuration of the Stealth Biplane. Data for the finite wing shows the high maximum lift coefficient and the broad angle of attack range capable of the Wortmann. In the right figure, however, lift has been corrected for the aspect ratio of the two wings and the drag curve reflects the addition of drag induced by the wings. From this figure it is apparent

² The Design of the Aeroplane, Darrol Stinton, Van Nostrand Reinhold Co., 1983.

that a large loss of lift and a large increase in drag (especially at high angles of attack) can be expected from the finite wing.

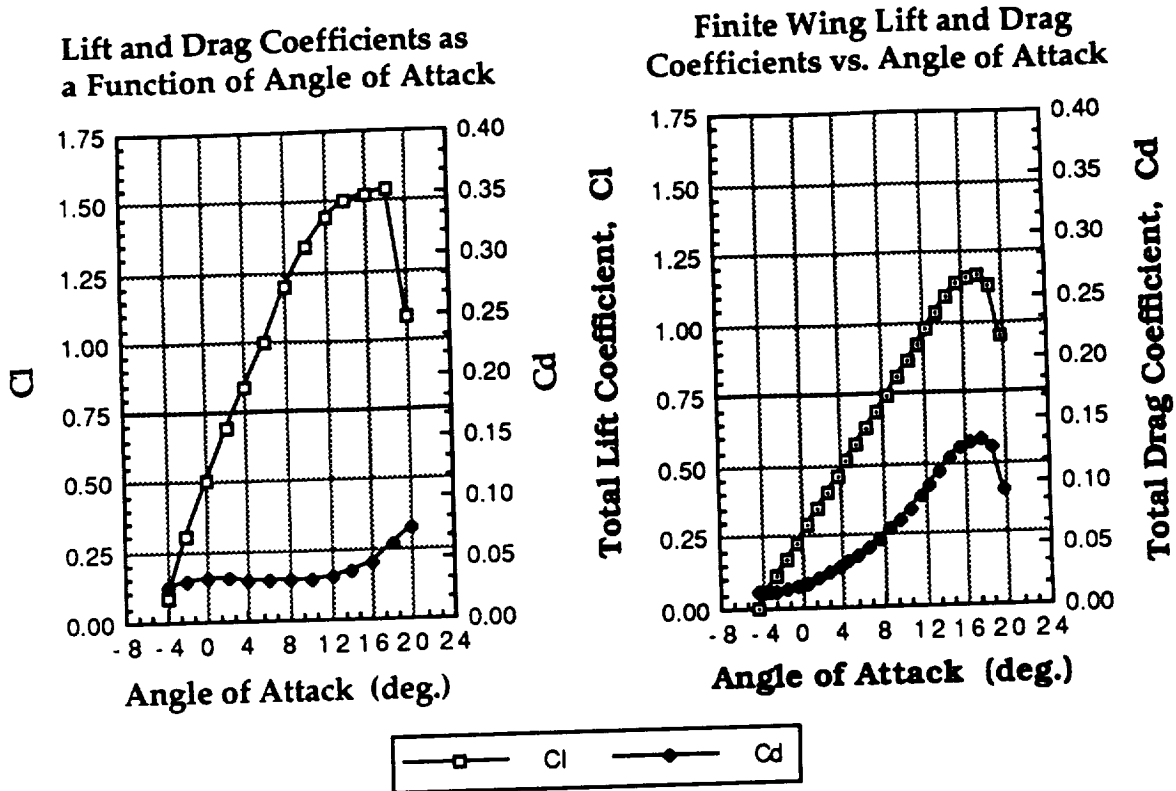


Figure 2

Fuselage Design

The fuselage for the aircraft was based on the requirement that it have sufficient volume to hold electronic systems whose smallest dimension is two inches. A long, slender fuselage shape was desired in order to keep profile drag low and combine the functions of carrying payload and connecting empennage to the forward structure. Thus a long, box-like, balsa structure was developed for minimum internal volume and ease of construction. The use of a cylindrical fuselage would result in less drag, however, internal systems and electronics mounting, cylindrical frame construction, and wing mounting would be much more difficult.

It must be noted that the aircraft's Silver Streak engine is not mounted inside the fuselage. Due to the heat generated by the engine, it requires a mechanism for keeping it cool. Rather than allow limited airflow through the fuselage, the engine is mounted outside the fuselage in front of the nose providing maximum airflow and thus cooling while not adding the weight of a full cowling or extension of the fuselage. This is more fully covered in Cowling Addition and Engine Cooling.

The payload-carrying section of the fuselage does not extend the full length of the fuselage. All payload and electrical systems are carried in the forward section of the fuselage with the remaining length consisting only of a small cylinder structure made of balsa. The cylinder structure simply connects the tail to the rest of the aircraft and carries the moment forces between the two. The 4-gram cylinder alleviates the need to construct a large truss structure while providing the same, if not more rigidity, as a truss.

Drag Prediction

The biplane's drag characteristics were evaluated by developing a drag polar for the entire aircraft. Since the major parts and characteristics of the Stealth Biplane are known at this stage in the design, a fairly accurate prediction of the drag of the aircraft can be made.

The drag of the aircraft was determined from a drag prediction method which evaluates the parasitic and induced drag through a simple aircraft breakdown technique referred to as Method II -- Preliminary Estimate ³. The total drag is divided into three sources as shown in the equation below

³ A Drag Prediction Methodology for Low Reynolds Number Flight Vehicles, Dan Jensen, University of Notre Dame Master's Thesis, January 1990.

$$C_D = C_{D0} + C_{Dp} + C_{Di}$$

where C_{D0} is the parasite drag coefficient of all aircraft components except the wing, C_{Dp} is the parasite drag coefficient of the aircraft wings, and C_{Di} is the induced drag of the lift produced by the wing.

Using the aircraft breakdown technique, drag coefficients are determined for each component of the aircraft based on the shape of the component and the boundary layer condition of the flow over the component. In addition, a form factor is computed for each component to account for the effect of its shape on the pressure distribution and thus the drag. In this way, the parasite drag coefficient, C_{D0} , of all the aircraft components except the wing are found from the equation

$$C_D = \sum \frac{C_{f_\pi} FF_\pi S_{wet \pi}}{S_{ref}}$$

where C_{f_π} is the skin friction coefficient of the component, FF_π is the form factor of the component, $S_{wet \pi}$ is the wetted surface area of the component, and S_{ref} is the reference area taken to be the total wing surface area of the biplane.

Relations for obtaining the induced drag coefficient must be modified, however, since this is a biplane design with special induced drag and interference characteristics. For biplanes, Max Munk developed a special relation for induced drag ⁴:

$$C_{di} = \frac{S C_l^2}{2b^2 \pi e} (1 + \sigma)$$

⁴ The Design of the Aeroplane, Darrol Stinton, 1983 Van Nostrand Reinhold Co., p. 157.

where b is the average of the two wing spans, S is the total lifting surface area, $\sigma = 0.5$ for most biplanes, and the span efficiency for the Stealth Biplane is estimated to be 0.85.

Thus, writing the total drag more explicitly

$$C_D = \Sigma \frac{C_{f_\pi} F F_\pi S_{wet} \pi}{S_{ref}} + C_{Dp} + \frac{S C_l^2}{2b^2 \pi e} (1 + \sigma)$$

From the preceding relations, the drag polar was calculated and the results depicted in the figures below (figure 3). The procedure for calculation and the results for the Stealth Biplane are given in detail in Appendix D - Drag Calculations. The figures below show the differences in drag characteristics between the infinite wing and the entire aircraft. Since the actual aircraft must use a finite wing, the maximum lift is greatly reduced. In addition, the figures show the change in profile drag with the inclusion of the fuselage and empennage. When considering the rest of the aircraft, the parasitic drag coefficient increased approximately 38%.

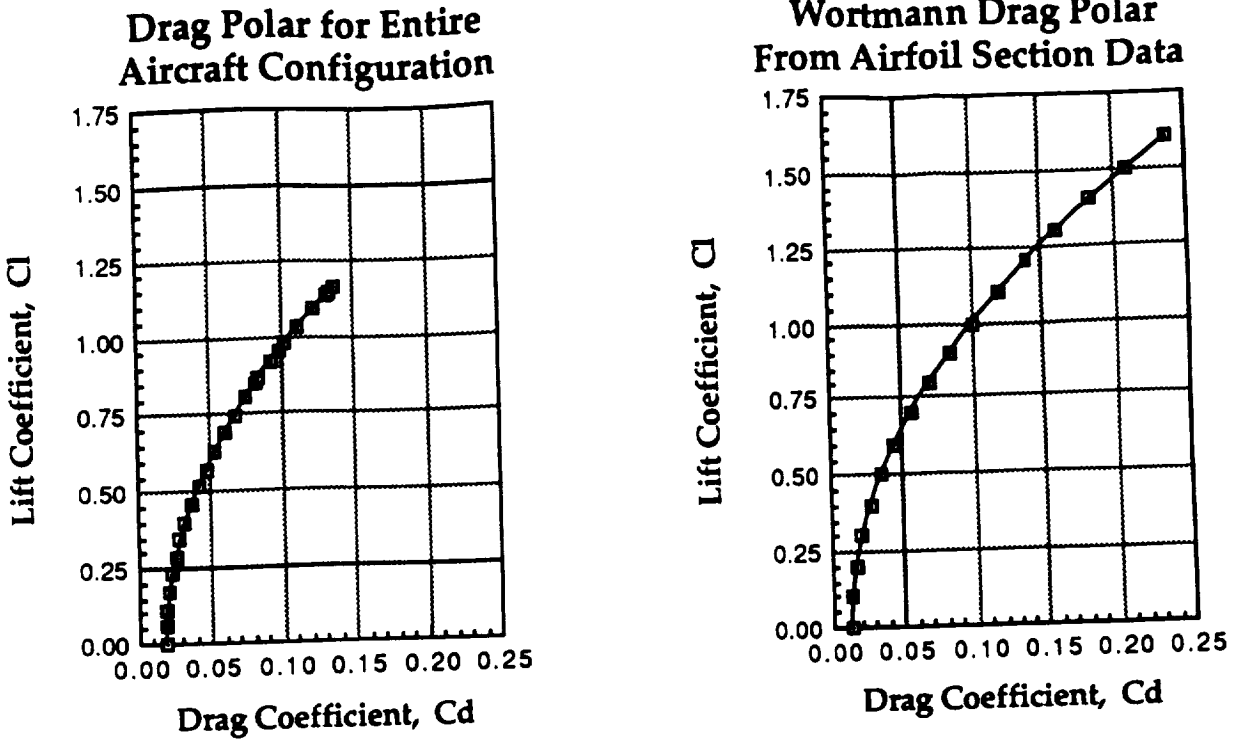


Figure 3

It was stated previously that a fairly accurate drag prediction can be made with the characteristics of the major aircraft components known. This is true, however, the method used here may be inherently inaccurate. The regime of applicability for this method is for vehicles operating at a chord Reynolds number between 10^5 and 10^6 and Mach numbers between 0.05 and 0.30. In addition, it is recommended that this method be used only for "conventional" configurations with moderate sweep and higher aspect ratios ($\Lambda < 35^\circ$ and $AR > 4$)⁵. The Stealth Biplane falls within all of these constraints (after modifying the induced drag for a biplane) except for the flight Mach number regime. With a cruise velocity of 28 ft/s, the Stealth will be operating at approximately 0.025 Mach. Yet, even though this is out

⁵ A Drag Prediction Methodology for Low Reynolds Number Flight Vehicles, Dan Jensen, University of Notre Dame Master's Thesis, January 1990.

of the regime of applicability, the results are assumed to be very close to the actual drag.

Gap and Stagger

Stagger is the relative position of two or more wings in which the leading edge of one is located forward of the leading edge of another not in the same horizontal plane. Originally, biplanes were built with wings placed directly over one another in a box kite fashion. Since the air deflected downward by the upper wing had a tendency to destroy the lift of the lower wing, staggering was introduced.

The interference between wings is reduced by staggering. Lift and efficiency increase materially with positive stagger (upper wing forward of lower wing) but negative stagger *reduces* lift and in most cases efficiency. It has been found that when wings are staggered 40% of the chord, both lift and efficiency increase by 5%⁶. In staggering the wings it should be borne in mind that the greater the stagger, the farther apart the individual centers of pressure are moved, thus increasing the moment created by the two wings. This was validated by varying stagger using computer models, where a stagger of 0.4c increased the overall moment coefficient by 40-50%. For the Stealth Biplane, the wings are staggered 40% of the chord, yielding an upper wing placed 3.2 inches forward of the lower wing.

The gap between two airfoils also affects efficiency and lift. While structurally it would be more convenient for the wings to be close, the closer they are the less lift is produced as a combination, and efficiency is reduced. While practically no loss of lift and efficiency could be achieved for

⁶ Grant, Charles H., Model Airplane Design and Theory of Flight, J. J. Little & Ives Co., 1941.

a gap equal to 3 times the chord⁷, it is inconvenient to combine wings with a gap to chord ratio greater than 1.5 from a structures and drag standpoint. For the Stealth Biplane, the gap was chosen to equal the root chord -- 8 inches.

Propulsion System

Propulsion System and Airframe Integration

From the geometry and balance characteristics (center of gravity and thrust), the Stealth Biplane requires a single powerful engine mounted at the front of the fuselage. Both the top and bottom wings will be indirectly affected by the wake created by the spinning propeller, however, this will not have a large adverse effect on wing performance because of the distance between the propeller and wing. The fuselage will not interfere with the wake created by the propeller, because it has been designed only slightly larger than the diameter (1.5 inches) of the Stealth Biplane's engine. Adequate control of the biplane is provided by the rudder and elevator.

⁷ Grant, Charles H., Model Airplane Design and Theory of Flight, J. J. Little & Ives Co., 1941.

(utilizing only two servos for reduced total aircraft weight) and the empennage is far enough away from the propeller and not in either plane of the biplane's wings to ensure aircraft stability and responsiveness. A small, tapered cowling with cooling intakes will provide enough ventilation to the internal parts (consisting of the Stealth Biplane avionics) of the solid balsa wood fuselage (through the entire fuselage) to eliminate any overheating problems.

Consideration of Parameters and Constraints

Fixed design parameters for the propulsion system include power available, design speed for the engine, and thrust available. Variable design parameters which influence the selection of the propulsion system include aircraft velocity, weight, propeller efficiency, electric motor RPM, endurance, load torque, and power drain.

Constraints for the propulsion system selection include minimum thrust and power required derived from the general environment (density, kinematic viscosity at 860 feet above sea level) and the minimum aircraft specifications (aircraft efficiency, aspect ratio, span, velocity, vertical and horizontal load factor, weight, lift developed, parasite and induced drag coefficients, and propeller efficiency, diameter, and advance ratio).

Power System Selection

To decide which type of non-airbreathing propulsion system was necessary to fulfill all of the mission requirements, a power required (and power available) versus velocity curve was constructed (see figure 4 below).

Power Available and Power Required vs. Velocity

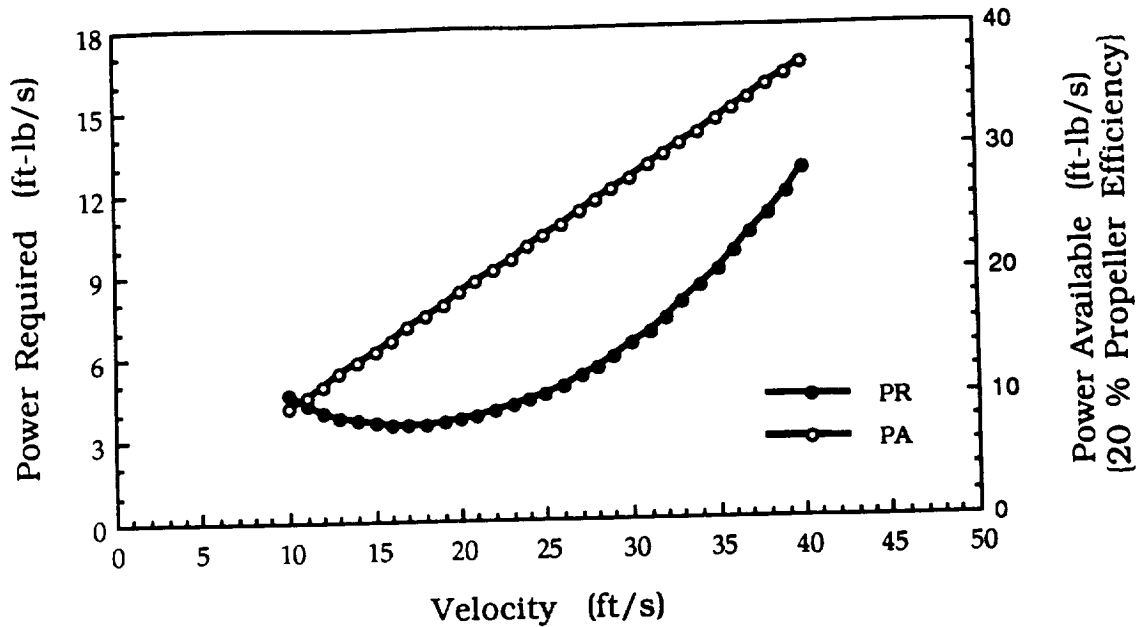


Figure 4

From this graph, (utilizing idealized equations found in Appendices A, B, and C) a power required of approximately 6 ft-lb/s (8 watts) is necessary for the aircraft to cruise at a mission velocity (Reynolds number of 100,000) of 28 feet per second. Studies of various aircraft power required segments of the mission indicate that the highest power required is during the take-off phase. The power required by the biplane to cruise at 6 ft-lb/s (8 watts) may be practical for the cruise segment of the flight, but from the limited data collection on this phase of the mission (specifically take-off performance), the estimated power required for a non-ideal takeoff (must include the effects of gravity, boundary layers, and aircraft manufacturing and machining imperfections) greatly exceeds this cruise power required by almost 10 times. Therefore, the power required (estimated at almost 80 watts) and the power available at the take-off segment is the most dominant

part of the selection process for the propulsion system. The Stealth Biplane must be able to take off in less than 75 feet and climb to a cruising altitude of 20 feet with sufficient power (available) remaining to complete the required mission of 3 laps and a landing (either power-off or the electric motor idling). Various propulsion systems considered include an electric motor, a wound rubberband/elastic torque producing system, a ducted fan (similar to the electric motor, but with a shell placed just outside of the diameter of the propeller), and carbon dioxide (gas driven engine, both direct gas thrust and modified gasoline to carbon dioxide) were studied, with the important results (from a previously performed propulsion system parametric trade study) listed below.

The rubberband/elastic propulsion system is generally employed with RPV gliders because of the elastic systems' short endurance, high (but not constant) maximum power output, low cost, and light weight. The reasons that the elastic propulsion system is not appropriate for this mission design include: the very high torque or moment demands on the fuselage structure with wound rubberbands (required high structural bracing and high bracing weight), uncontrollable and non-constant (varying as the elastic unwinds) power output, low (relative to gas or electric) power, and overall short system endurance. Some of the best (thickest and most elastic) wound rubberband systems can produce varied power for up to 40 seconds, but for this mission Reynolds number of 100,000, and the payload and avionics system demand a longer endurance and higher power available.

A ducted fan propulsion system was considered because of the benefits in reduction of propeller tip vortices, and a corresponding reduction in propeller wake turbulence. However, a large diameter propeller is required to provide enough static thrust to taxi, rotate, and lift the Stealth Biplane to

the desired altitude, and an eight inch diameter ducted fan does not fit in with the small 6.5 in² cross sectional area fuselage selected, wing design, and overall aircraft geometry. A smaller ducted fan does not produce enough power for take-off, and does not mesh with the Stealth Biplane's mission requirements.

Carbon dioxide propulsion (both direct jet thrust with a nozzle and modifying a reciprocating gas engine to carbon dioxide 'fuel') was eliminated as a propulsion system choice because of four factors: 1) the gas is actually emitted (hence a change in mass of the aircraft - violating one of the mission specifications), 2) a large volume of compressed CO₂ gas is necessary to complete the mission, 3) speed control for take-off and cruise is difficult without complicated gas ducting and throttling hardware, and 4) the modifications, selection, and availability of CO₂ engines is very limited and difficult.

Electric motors provide dependability, variable speed control, and relatively high endurance for non-airbreathing engines. A limitation of electric motors is the low thrust to weight ratio as compared to similar sized gasoline motors. Because gasoline motors are not a viable consideration (change in the weight of the aircraft from the burned fuel, violating a mission requirement), the best propulsion system available was the direct current electric motor. The determination for the best electric motor was based on the following parameters: weight, power available, battery power drain, and endurance. A comparison of electric motors (see Figure 7) shows various electric motors and their system weights.

The Peck Silver Streak 035M (modified) definitely outperforms all of the other electric motors studied in all of the important performance categories, while remaining much less expensive to purchase. The data

from the power required and power available versus velocity curve suggests the selection of a light electric motor with no gearbox (gearboxes lower the propeller RPM, decrease the engine effectiveness by adding a torque to the motor line of thrust, and add significant friction losses). A large propeller placed on a small motor will slow the engine designed rpm down to the equivalent of a large motor with a gearbox. Significant engine and battery heating will occur in the small engine as the load torque increases, but with an adequate air cooling system installed, this heating will not cause motor damage. The Peck Silver Streak 035M was tested for 4 minutes at full throttle (the complete mission - take-off, rotation, climb-out, 3 figure eight laps and landing - requires approximately 2.5 minutes) to ensure sufficient engine endurance. The versatile Silver Streak 035M was selected for the Stealth Biplane on account of its low weight of only 2.6 ounces, small size (diameter of 1.09 inches and length of 1.50 inches), and large power (available) output of 95 watts. The power available was computed two different ways: by the coefficients of thrust, torque, and power and by using the Motor Data Sheet developed by the computer program CTCQCP (Refer to Appendix C). This Motor Data Sheet utilizes three main parameters: load torque, motor amps, and motor RPM to compute a number of important data results including power available. The graph shown in Figure 5 was generated with a propeller size of 8 inches (size 4 pitch) and an engine rpm of 9,000 rpm.

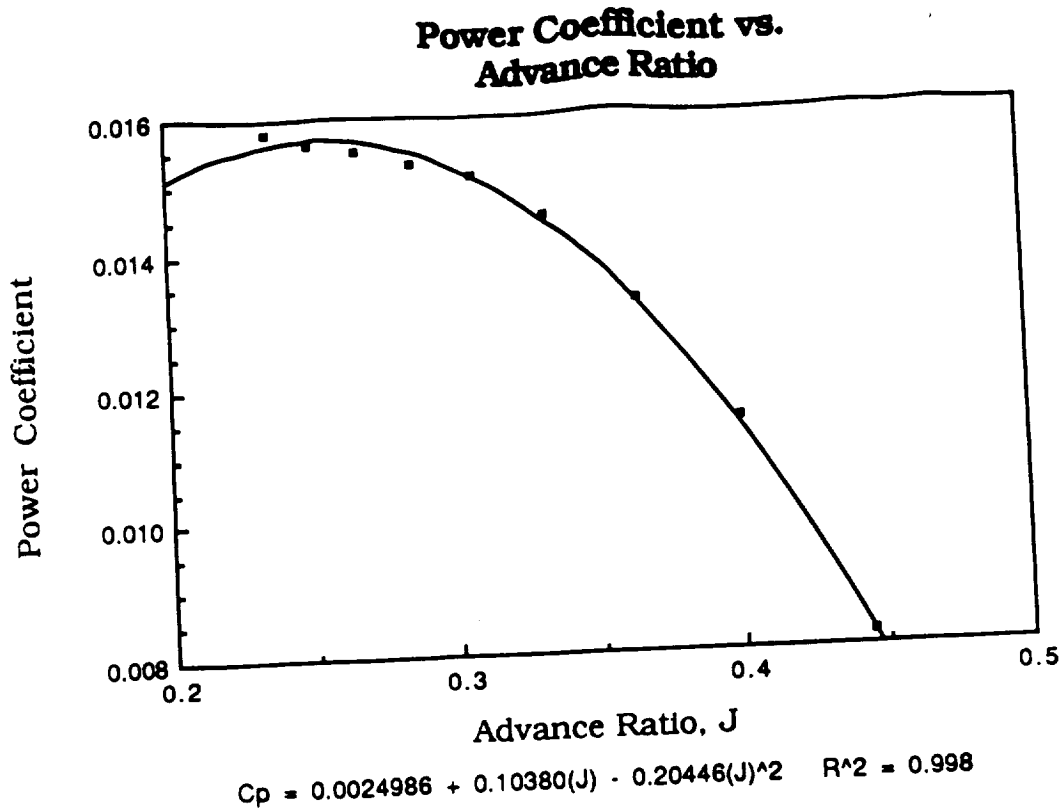


Figure 5

The equations for the coefficients of thrust and power versus J (set constant, determined by the velocity, propeller diameter, and revolutions per second) curve fitting were entered directly into RPV Preq Eng Program (See Appendix A).

The method of using the Motor Data Sheet requires selecting a propeller, determining the engine RPM and then computing the load torque placed on the motor by the propeller. After determining the operating load torque, simply read across the graph to the corresponding power available. Another method of computing the power available is to continue with the computer code KTFTEW (Kevin T. Flynn '90, Timothy E. Walsh '90) listed in Appendix B. This program, developed specifically for the Peck Silver Streak 035M electric motor, determines the load torque, and power and thrust

coefficients. The graph shown in Figure 6 was generated with a propeller size of 8 inches (size 4 pitch) and an engine rpm of 9,000 rpm.

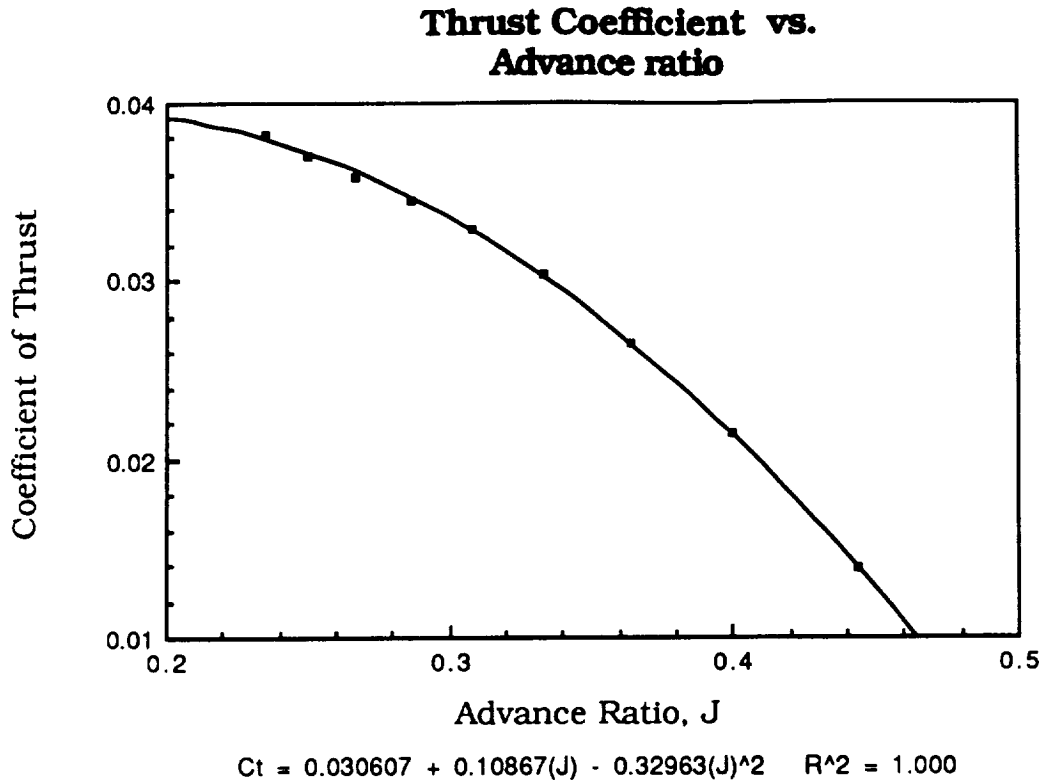
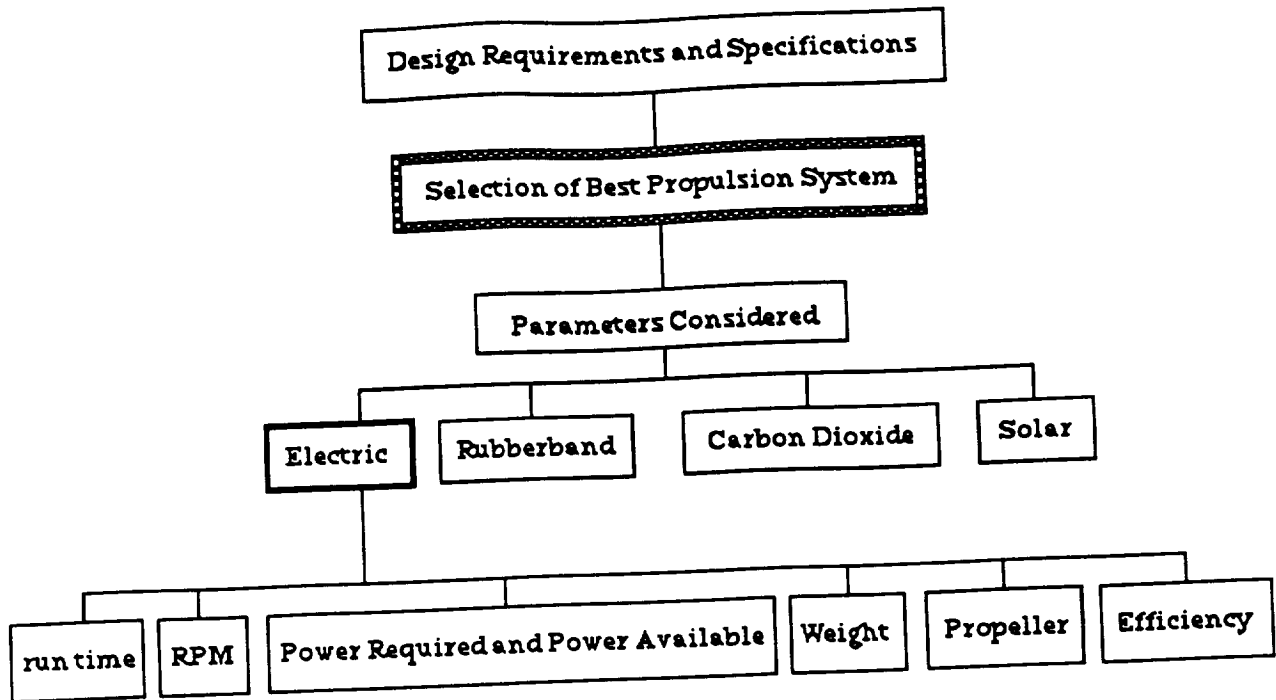


Figure 6

The power available data developed from these different systems were very similar, averaging out to approximately 95 watts. Another method that was used to check the accuracy of the power available was by placing the 035M engine in a test stand. The static thrust developed by the electric motor was measured at approximately 12 Newtons, and if a crude relationship ($P_{avail} = T \cdot V_{cruise}$) is employed, the power available is approximately 100 watts. The problem with this assumption lies in the fact that thrust decreases as velocity increases, but it is still good engineering judgement to actually test components before using them, even if accuracy is limited.

Flowchart for the Aircraft Propulsion System Selection



Electric Engine Specifications

<u>Motor</u>	<u>Motor Weight</u>	<u>System Weight</u>	<u>Direct RPM</u>	<u>Geared RPM</u>	<u>Power Available</u>
A 020	3.5 oz	9 oz	6x4 10,000	10x6 4,500	50 watts
A 035	4.5 oz	12 oz	6x4 13,000	10x6 6,000	90watts
A 050	6.5 oz	16 oz	7x4 14,500	11x7 6,500	125 watts
A 150	7.5 oz	25 oz	7x4 16,000	11x7 7,500	200 watts
SS 035	2.6 oz	7.4 oz	6x3 10,000	only direct	48 watts
SS 035M	2.6 oz	10 oz	8x4 11,000	only direct	95 watts

"A" designates Astro Flight System "SS" designates Peck Silver Streak
 "M" denotes Modification; addition of batteries
 The propulsion system weight includes the harness and the electronic switch.

Figure 7

Propeller Selection

The propeller selection is directly dependent on the engine selection, and after comparing the power required and power available curves versus the propeller diameter of the Stealth Biplane and the Silver Streak 035M electric engine, as well as performing numerous experiments on a (ball bearing) mechanical spring static thrust test bed, an 8 inch diameter propeller with a 4 inch pitch was selected. The 4 inch pitch was determined from our Reynolds number and RPM, and limited by the amount

of load torque (and motor amps) that the Peck Silver Streak 035M electric motor could produce. A six inch pitch propeller places too much load torque on the motor (observed by excessive heating of the motor after a static test) which suggests the selection of a 4 inch pitch propeller. The power required to fly the biplane and power available provided by the motor selection curves (see Figure 8 below) versus propeller diameter (both power available and power required are functions of the advance ratio, J) was developed from a simple computer code RPV Eng Preq (Kevin Flynn '90) (see Appendix A) and TK!Solver software (utilized as a cross check and reference), and the best airfoil shape and pitch for the propeller were determined by using Clark-Y and Wortmann airfoil comparisons. From this graph, the obvious choice for the propeller diameter is in between values of 7 and 9 inches, and the middle value of the 8 inch diameter propeller was selected. Also used was a program from AE454 Propulsion (written by Timothy E. Walsh '90 and Kevin T. Flynn '90) (see Appendix B) which determines the idealized performance of an aircraft and selected propeller. This program, KTFTEW, models three different aircraft (this program varied aircraft efficiency) and three different propellers (Zinger, Airscrew, and Topflite) to determine the best Stealth Biplane combination. From the propeller efficiency versus advance ratio graph (see figure 9), a propeller efficiency of 0.54 can be determined.

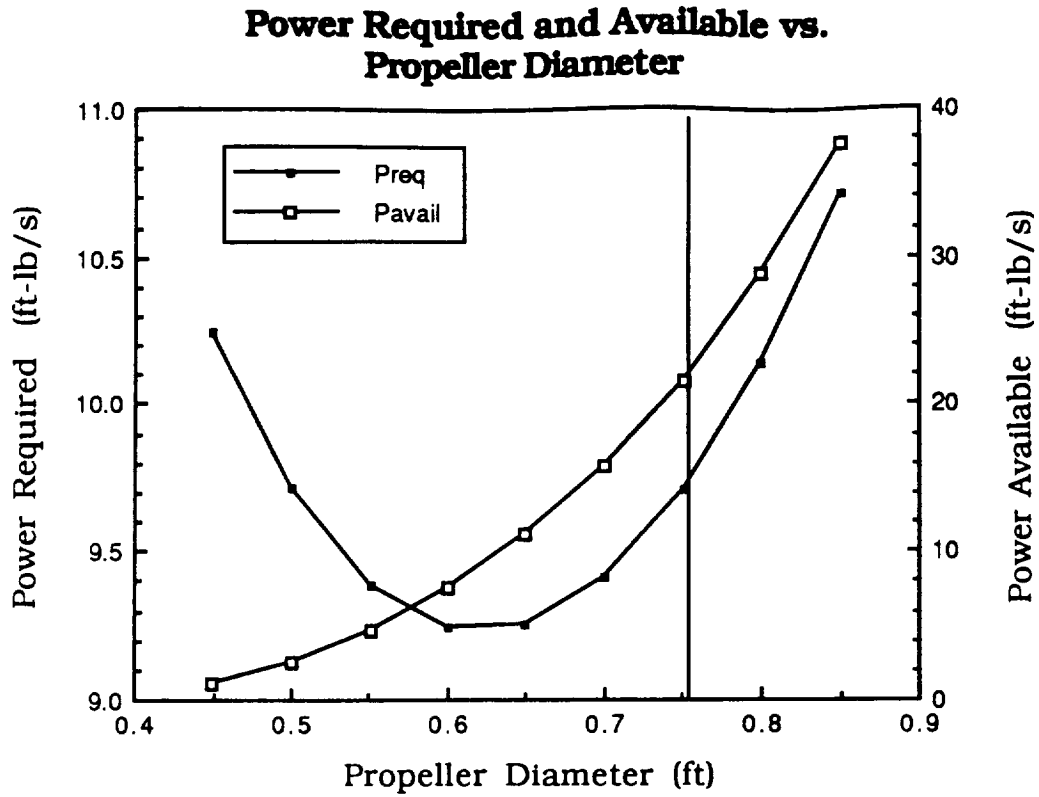


Figure 8

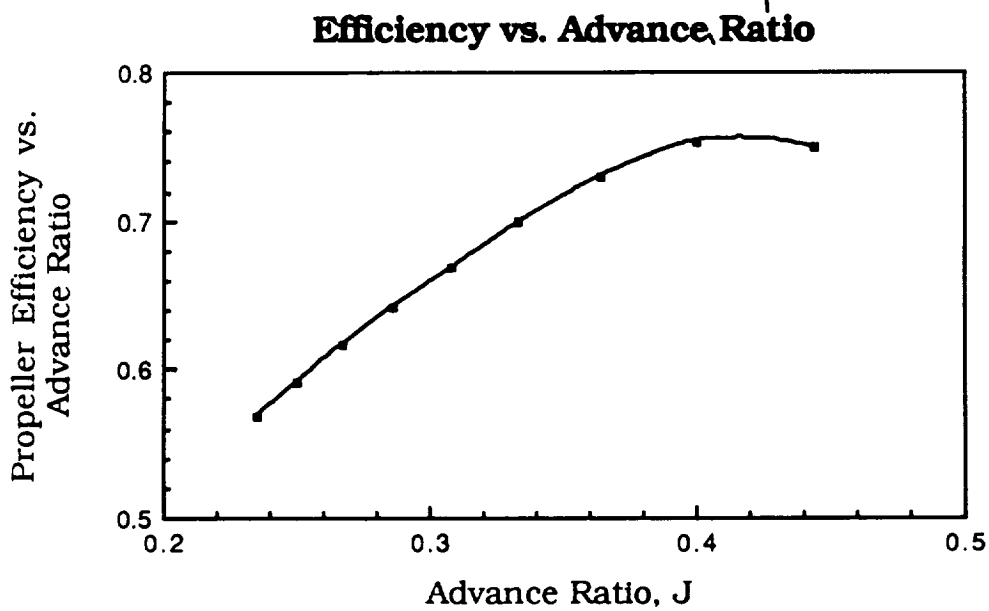


Figure 9

From these computer programs (see Appendices A, B, and C for computer codes) and the compiled static thrust test stand results, the *Rev* -

Up 8 x 4 propeller was selected as the propeller that will most effectively accomplish the mission.

Number and Size of Batteries

The Silver Streak is an advanced polymer general purpose (utilizing magnets and brushes) electric motor designed to operate with 6 AA 1.2 Volt, 600 mAh Nickel-Cadmium batteries (maximum power output of 47 watts with a 6 x 3 propeller). By increasing the number of batteries to 10, the maximum power available goes up to 95 watts. Six batteries (weighing 4.8 ounces) were suggested by the manufacturer of the engine to run the SS 035M at 48 watts, but with the addition of a larger propeller, an increase in the load torque requires more batteries. Because the electric motor selected is a general purpose motor, the number and size of batteries can vary for each specific design requirement. The number of batteries (total of 10, weighing 8 ounces) increases the static engine power of the SS 035M (modified) to 95 watts. This number was determined by the process described in the aforementioned section and a crude check (using a test stand to deflect a mechanical spring a certain measured distance, and then weights applied to deflect the spring the same distance) obtained a static thrust result of almost 12 Newtons. Although this number is a static value, a very general check of theoretically computed values of power available can be performed. Multiplying the static thrust by the cruise velocity of 8.35 m/s (27.4 ft/s) yields the maximum power available of 95 watts. Results from the static thrust tests indicate a parabolic curve (see Figure 10), which shows that the best performance of the electric motor and matched propeller is found when ten AA batteries are employed in a series configuration, yielding 12 Volts and 600 mAh.

Non-rechargeable batteries were considered as part of this mission, but the cost for 10 AA non-rechargeable batteries would exceed the cost for rechargeable batteries after only 2 complete missions and no tests. The single most important factor considered when selecting the number of batteries is the power available during the take-off phase of the mission. The completion of the mission depends on the aircraft successfully rotating in less than 75 feet and ascending to the cruise altitude of 20 feet. Initial calculations from the KTFTEW computer code indicate the Stealth Biplane should rotate in approximately 40 feet, and climb to the cruise altitude of 20 feet in approximately 100 feet. The internal cross-sectional area of the fuselage limits the size and configuration of the battery pack, and the critical minimum weight design of the Stealth Biplane limits the weight of the propulsion power pack. Therefore, 10 small AA 1.2 Volt, 600 mAh rechargeable Nickel-Cadmium batteries were selected for the battery propulsion system.

Engine Speed Control

For the specified mission, the power required at take-off of over 30 ft-lb/s (40 watts) compared to the power required for cruise of 6 ft-lb/s (8 watts) emphasizes the need for variable engine speed (which varies voltage for RPM and current for load torque), and this is added to the propulsion system in the form of a speed controller. The speed controller is a fused (25 amps) array of capacitors and assorted electronic equipment that controls the engine RPM (and the corresponding current and power drain) of the battery pack from stopped to full speed (12,000 RPM). Engine speed, therefore, is

Measured Static Thrust vs. Number of Batteries

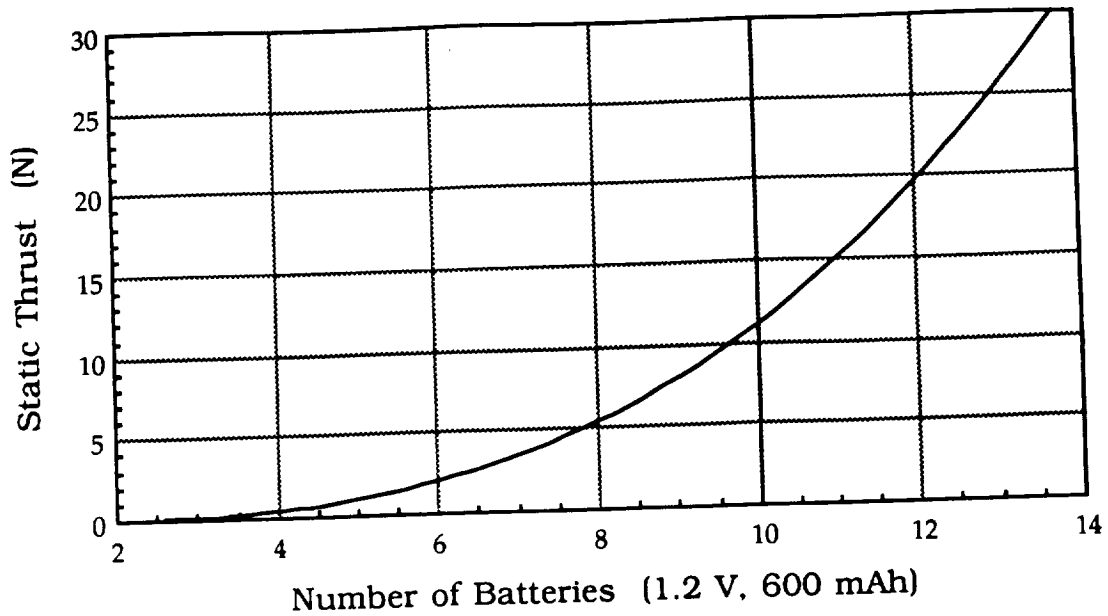


Figure 10

completely controlled by the Stealth Biplane remote control pilot. The propulsion system weight (see Figure 7) is increased by adding the speed controller, but the Nickel-Cadmium batteries have a constant current drain, and the speed controller is justified. A heat sink is attached to the speed controller to lower the heating problems, and cooling the controller with airflow through the fuselage is accomplished by placing the heat sink directly in the middle of the ventilated fuselage.

Engine Placement

Engine placement was studied in detail to determine the where the engine would operate most effectively, and the placement of the engine in the front of the aircraft ensures an effective static thrust line (very small moment from the fuselage reference line), and adequate cooling and center of gravity placement. The tractor (puller) configuration in the fuselage of the Stealth Biplane (tail dragger) was selected as the best place for the Peck

Silver Streak 035M to keep the propeller from making contact with the ground. The low back wheel (connected to the rudder) significantly raises the front of the biplane while reducing the length of the main gear. A tricycle gear aircraft would lower the propeller operating arc (propeller diameter) and decrease the Stealth Biplane performance, which is why the tail dragger configuration was selected with the propeller in a puller position.

Cowling Addition and Engine Cooling

The addition of a small cowling streamlines the transition of a 1.09 inch diameter electric motor fitted to a 2.1 inch by 2.1 inch fuselage. The 4 in² (2 in. by 2 in. inner dimensions) internal area of the fuselage was specified in the mission requirements (2"x2"x2" payload weighing two ounces), and the cowling was added to effectively transition the electric motor diameter to the fuselage while virtually nullifying the effects of fuselage blockage (very little static thrust impeded or lost by this design).

Conclusion:

Peck Silver Streak 035M Electric Motor	2.6 ounces
8 x 4 Rev - Up wooden propeller	0.3 ounces
10 Nickel Cadmium AA 1.2 V, 600 mAh for motor	8.0 ounces
RPM Speed Controller	2.4 ounces
Radio Control System	1.2 ounces
2 Futaba MR1245 Servos	1.2 ounces
4 Nickel Cadmium AAA 1.2 V, 400 mAh for receiver	<u>2.8 ounces</u>
Engine placement in the front of the fuselage	Sum = 18.5 oz.
Tapered cowling to front of engine	<u>Add payload + 2.0 oz.</u>
Total Stealth Biplane Avionics and Payload	Sum = 20.5 oz.

Performance Estimation

Takeoff and Landing

For any flight vehicle, takeoff is invariably one of the most critical portions of the mission. Flying at maximum conditions, the aircraft typically operates very near its stall velocity while rotating towards its climb-out angle of attack. Once the aircraft leaves the ground and climbs towards its cruise altitude, it leaves the friendly confines of ground effect and thus must rapidly provide even more lift. While all this is occurring, the entire vehicle can be subject to severe flight conditions such as wind shear, unsteady air, or sudden cross-winds. These natural phenomenon can quickly stall the airplane and send it crashing to the ground before the ground based pilot can even react; therefore, it is imperative that the takeoff portion of the flight be supplied not only with ample takeoff power, but also extra power available in case of flight disturbances. The Stealth Biplane must be able to takeoff and climb to its cruise altitude (20 feet) in a distance of 150 feet.

Calculating the ground roll distance for an aircraft is not terribly difficult, yet also not totally obvious. The takeoff performance for the Stealth Biplane has been estimated by the construction of a computer code which is capable of estimating, along with other quantities, the ground roll distance required for takeoff as a function of engine power. Once the ground roll distance has been determined, the climb angle can be found by geometry since the desired altitude at the end of the runway is known (20 feet). The following figure (figure 11) shows ground roll distance and climb angle plotted versus engine power required.

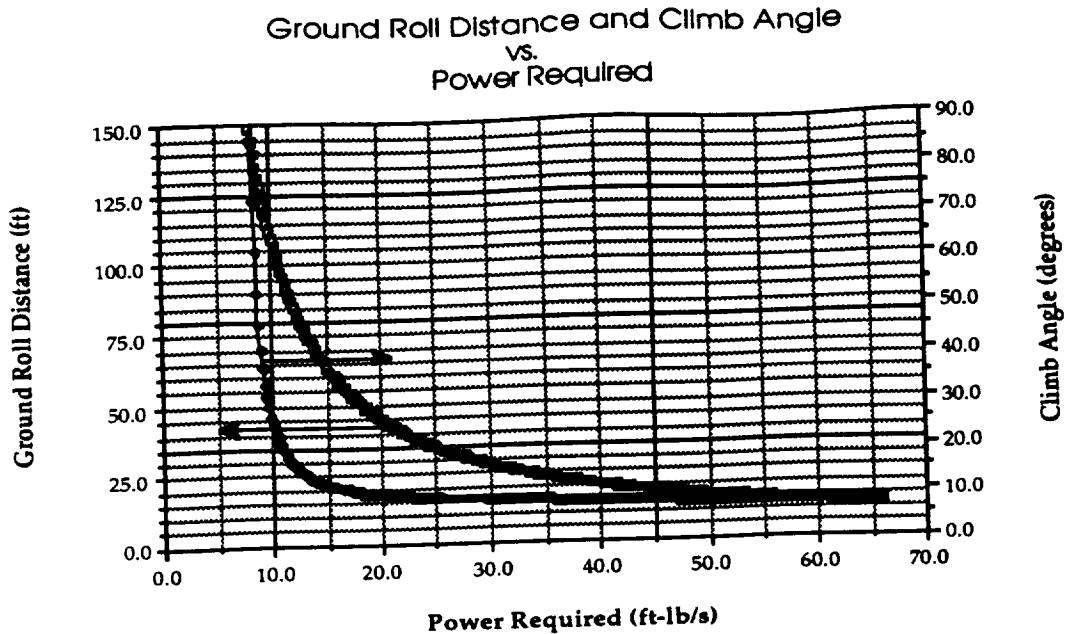


Figure 11

For our flight plan, we estimate the Peck Silver Streak 035M powerplant will be able to get the aircraft to its takeoff velocity (30.5 ft/s) in a ground roll of approximately 50 feet. This would dictate a climb angle of 11 degrees to reach its cruise altitude. This type of climb to altitude necessitates a rate of climb of 350 feet/min.

The landing calculations are made in a fashion very similar to that of takeoff. During the landing run, the aircraft will be operating at its maximum angle of attack of 14° . Knowing the lift curve slope and correcting for aspect ratio, one finds that the total lift coefficients for the top and bottom wings are 1.25 and 1.15 respectively. Providing that the top wing contributes 52% of the total lift and the bottom wing gives 48% of the total lift¹, the total lift coefficient for both wings is about 1.20. Consulting the drag polar for the aircraft (see section on Drag Prediction), the (L/D) shows

¹ Grant, Charles H., Model Airplane Design and Theory of Flight, J.J. Little and Ives Co., New York, 1941.

a value of 8.6. For an unpowered landing, this would give a glide angle of 6.6° . Thus, to bring the aircraft down from its cruise altitude of 20 feet, the Stealth Biplane should glide for approximately 170 feet after powering off. This poses a definite problem for the landing regime mainly because the runway measures only 150 feet in length. If the Stealth were to touchdown one quarter of the way down the runway, the landing run from the cruising altitude would have to begin 130 feet downrange of the threshold; not within the confines of the mission course. Therefore, the only feasible solution is to start the landing run at a lower altitude.

For a proper touchdown, this would require a landing run starting height of 13 feet. The only other solution would be to actively point the aircraft toward the ground, instigating a dive, and pull up at about an altitude of 5 feet. However at this altitude, ground effect and excessive velocity would cause the aircraft to tend to regain altitude, or "balloon" over the runway. In "real world" applications, this undesirable landing problem can be conquered by deploying trailing edge flaps or leading edge slats, which effectively increase the camber of the airfoil and allow slower landings. Yet, for this design, weight and servomotor constraints negate this solution. It will inevitably take a skilled pilot to land the Stealth Biplane.

Range and Endurance

Since the course length of the mission is fixed (approx. 2250 feet), range is not of paramount import. However, in a manner that will be shown in further detail when endurance is considered, the maximum range of the Stealth Biplane is estimated to be 7140 feet (1.35 statute miles) with a cruise velocity of 28 feet/sec. In regard to the mission, this easily exceeds the required range. This range would allow the Stealth Biplane to complete

the mission course roughly three times (9 laps). Taking into consideration additional required range for taxi, takeoff, loiter, and landing, the length of the entire mission would be closer to 3200 feet (1.5 times the mission course). Additionally, the aircraft's range can be further increased, with no weight penalty, by putting some of the batteries in *parallel*.

The battery pack used in the Stealth Biplane is made up of ten Ni-Cad batteries connected in series producing 4.25 minutes of usable thrust. Since the addition of batteries in series has no effect on the aircraft's endurance, a parallel configuration must be employed in order to change the endurance. Since ten batteries in series will produce much more endurance than is required for the mission, there is no need for the additional benefit of placing the batteries in parallel. A series configuration will give the maximum battery drain time while simultaneously supplying a maximum electromotive force, and therefore a maximum RPM, to the motor. All batteries mounted in parallel will give a maximum endurance configuration while simultaneously supplying a maximum current flow, and therefore maximum torque, to the motor. However, connecting all the batteries in the power pack in parallel, while giving maximum endurance, will most definitely not produce enough motor RPM to get the aircraft to takeoff, much less cruise. Thus, when considering lengthening the loiter time of the Stealth Biplane, a combination of batteries in series and parallel would have to be further explored. There appears to be no practical solution in shortening the 4.25 minute endurance time to fit a shorter mission scale, save the construction of a circuit board to lie between the speed controller and the battery pack.

Range and Endurance

Power Plant Configuration	Range (ft)	Endurance (min)
10 Batteries, in Series [†]	7140	4.25
10 Batteries, Series/Parallel combination ^{††}	35,700	21.25
10 Batteries, in Parallel ^{†††}	71,400	42.5

[†] Maximum RPM, maximum battery drain configuration

^{††} Acceptable RPM, decent endurance - 2 Series Sets, 5 parallel batteries each might pose takeoff problems due to loss of maximum RPM)

^{†††} Maximum Endurance, maximum torque (aircraft will be unable to takeoff in this configuration, much less cruise)

The above table summarizes possible battery configurations. The third configuration, as mentioned before, is impractical due to low RPM output. It is shown only for breadth as results from motor testing on the static test bed.

Structural Design

V-n Diagram

At the critical load condition, the load factor, n , was determined to be 1.5 while the negative critical n loading of the Stealth Biplane was estimated to be -0.5. The technology demonstrator was designed with these n loadings in mind. Due to the nature of the wing planform geometries and relative sizes, the bottom wing will invariably stall before the top wing. This is due to the downwash effects of the top wing on the bottom wing. Therefore, the lower wing, and thereby the entire aircraft, is predicted to stall at 22 ft/s. The stall velocity in a negative n loading was estimated to be 12 ft/s which was estimated from the $C_{l_{min}}$ of the airfoil. The maximum velocity attainable for the technology demonstrator was estimated by the propulsion team to be 40 ft/s and was designed to cruise at 28 ft/s. From the V-n diagram (figure 12), the load factors at these velocities are graphed as a function of velocity. The V-n diagram does not have a "never exceed" velocity in a dive limiting envelope. Due to the large factor of safeties existing for the technology demonstrator structure, a dive velocity for a maximum altitude of 25 ft will not cause any excesses in aerodynamic loading from a short dive from cruise altitude.

Load Estimation

Critical load estimation was determined from a takeoff condition. The worst case condition for the technology demonstrator will utilize the full length of the runway forcing a steep climb angle and rate of climb. The takeoff conditions are a 30.5 ft/s velocity with a 12 degree angle of attack. A computer program written on the PRIME computer taking into account the

V n Diagram

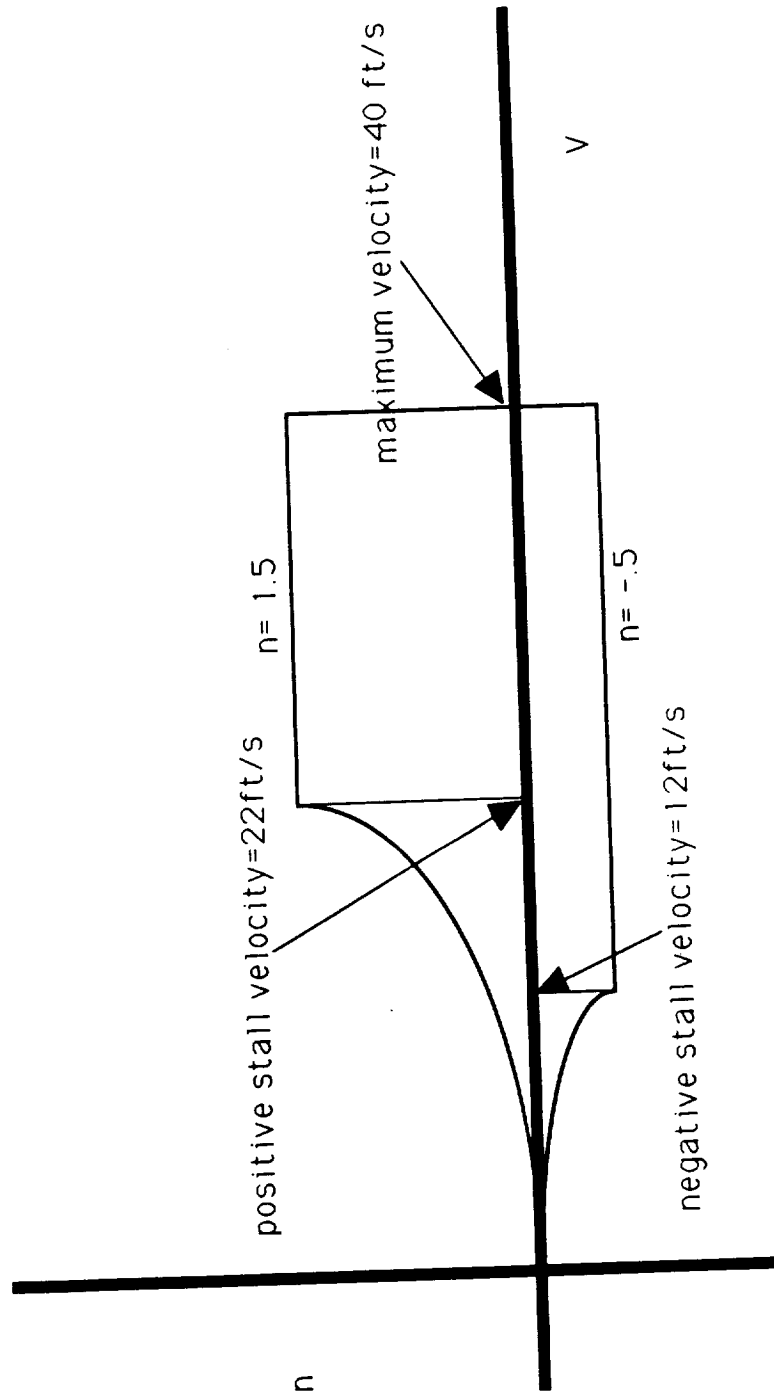


Figure 10

lift, moment, and drag distributions at the critical load was developed to analyze the shear and direct stresses at certain points on the wingbox structure and was programmed with this condition. The critical stresses on the wing were located at the centerline strut of the top wing. At the center line of the top wing, the worst case factor of safety in shear stress was 5.5. For load estimation at landing, the worst case factor of safety was determined through the use of basic force calculations. At a worse case, the aircraft will encounter a landing conditions of a 15 degree dive at 21 ft/s. Assuming the tire will deform approximately 1/2 inch. This will yield an landing impact force of 18.5 lbf in each wheel assuming only the front two main wheels hit the ground without bouncing. Only the main wheels are expected to bear the initial impact force of the landing. The tail gear will only be expected to absorb a very small percentage of the landing stresses.

Wing Structure

i) Introduction

Wing structure layout was decided based on wing designs of earlier technology demonstrators of the previous years. Earlier design groups encountered a harsher loading environment due to a more demanding mission requirement. The earlier design groups had aircraft that had flight regimes on the higher end of the velocity spectrum. As a result, the technology demonstrators were inherently heavy. Most of the technology demonstrators had the usual three spar configuration with spar caps. Rib caps and false ribs were also used to improve the airfoil shape holding ability of the wingbox structure.

ii) Top Wing Structure

The wings for the Stealth Biplane technology demonstrator will have a slightly different wingbox construction. For the top wing, the spars will be excluded. The spar caps will be sufficient in bearing the stresses. The main reason for the exclusion of the spar is for weight saving purposes. In addition, the load path of the lift forces from the wing will be distributed to three external struts mounted to the bottom of the top wing (see Figure 13), alleviating the demand for a spar. The spar caps will be made from 1/4 by 3/8 inch balsa, mounted at the top surface where the maximum thickness of the airfoil occurs. One is positioned at the leading edge which has the dimensions of 3/8 by 3/8 inch. Due to the sharp trailing edge of the airfoil, 1/16 inch balsa sheeting at the top and bottom surfaces will be used to reinforce the trailing area. The ribs for both wings are to be constructed from 1/8 inch balsa and the rib caps constructed from 1/16 inch balsa sheeting for the purpose of holding the airfoil shape.

The bottom wing will be constructed with the same wingbox construction as the top wing and will be mounted flush into the bottom of the fuselage box (see Figure 13). The bottom wing will be fastened by pegs strapped by rubber bands. The top and bottom wings will be built as a single unit so that during disassembly the top and bottom wings can be detached from the fuselage as one piece. The bottom wing will also bear the load path of the landing gear. The landing gear will be attached to the bottom wing at 5.5 inches from the fuselage centerline.

iii) External Strut Mounting

The external struts will be made from 1/4 inch by 2 inch plates cut to the shape of a symmetric airfoil. The outer struts are mounted 6 inches inboard from the wingtip of the top wing and are attached onto the wingtip of the bottom wing (see 3 View Drawing). The third strut is mounted at the

fuselage centerline and attached to the fuselage directly. The existence of external struts provide additional resistance to vertical wingtip deflections for both the top and bottom wing and also provide torsional resistance to both wings. With the structural reinforcement of the external struts, the internal structure of both wings may be reduced and lightened. As previously mentioned, the top and bottom wing will be a single unit. The Wing Unit can be detached from the fuselage during disassembly and transported in the allotted 2'x2'x4' shipping box.

iv) Computer Stress Estimation

The wingbox structure of both wings will be skinned with mylar. The wing skin of both wings will not hold any stress in compression loading. Stress analysis of the wings was done ignoring the effect of the mylar in tension loading, simply considering the positive load bearing capability of the mylar as a margin of safety. ASTROS, a finite element program written in FORTRAN on the DEC mainframe, however, did include the effect of the mylar skin on the wings but, it did not consider the changes in the load paths for a biplane when the external struts are introduced. Yet, the program did produce a rough estimate of the wingtip deflections for a biplane without external struts. The introduction of external struts will only decrease the wingtip deflections which was estimated to be one inch for the larger top wing.

The planform geometry of the wing was discussed in the aerodynamics section of this report. The wings will not employ any moveable lift or control surfaces. Lack of moveable surfaces enforces the rough estimates of the ASTROS program (see Fig.?????).

Fuselage Structure

The fuselage shape chosen was selected for ease in construction. The fuselage will have inside dimensions of 2"x2"x14" which will taper at the nose for the engine and at the transition to the tail boom and will be made from 1/4 inch thick balsa sheeting. The fuselage tail boom will be constructed from balsa having a hollow cylindrical geometry. It will have an outer radius of 1.5 inch, a thickness of 3/16 inch, and a length of 16 inches bringing the total length of the aircraft to 26 inches. The access door of the fuselage will be placed on the center third of the fuselage roof. The door will slide parallel to the wingspan for service. The centerline strut mount is located on the front third, close to the engine mount area. The area where the bottom wing will be mounted will have spruce pegs for the rubber bands which will strap the bottom wing onto the bottom of the fuselage. Mounting the wing by rubber band will also ease the preparation process of the technology demonstrator. The empennage will be made from 1/8 inch thick flat balsa plates for the control surfaces. The vertical and horizontal tail will be mounted onto a cross shaped base and the vertical tail will be attached to the top arm of the base. The horizontal tail will be mounted at one third the height of the triangular rudder for reasons of structural integrity and will be attached to the two arms of the base. The bottom arm of the cross shaped based will be embedded into the fuselage structure.

Materials Selection

Selection of the materials used in constructing the biplane was dependent on several important criteria. First, the material must be able to withstand the loads administered in normal and critical conditions and not fail. Second, the material must be of the lowest weight possible to keep the overall weight of the aircraft to a minimum. Third, the cost of the material should be reasonable to keep construction costs down. The material that best met these demands was selected.

As mentioned before, the aircraft material must be able to survive the array of loads placed on it. The aircraft, technically, has three regimes of flight where it will experience significant loads: takeoff, cruise, and landing. Takeoff best represents the critical load conditions. If the material can withstand these critical conditions, then it is suitable for selection.

At takeoff, the maximum lift condition will apply a total wing loading of 23.6 oz/ft². The wings were modeled as cantilever beams under these load conditions and the maximum axial stress for either wing was 411 psi. The fuselage, under critical conditions, experienced a maximum axial stress of 7.0 psi and a maximum torsional stress of 2.0 psi, while the cylinder portion of the aircraft experienced a maximum axial stress of 57 psi and torsional stress of 15 psi. The following chart gives the maximum axial and torsional stresses for different aircraft components under critical loads.

Results of Stress Tests for Different Components		
Structural Component	Max Axial Stress (psi)	Max Torsional Stress (psi)
Wings	411	-
Fuselage Box	7.0	2.0
Dowel	57.0	15.0

Different classes of materials were examined in choosing the proper material for the aircraft construction. They were judged on their performance in satisfying the material criterion of strength, weight, and cost. The different classes of materials examined were plastics, metals, composites, and wood. The chart below indicates the performance of the materials in the selection.

Performance of Materials			
Material	Strength	Weight	Cost
Wood	fair	excellent	good
Metal	good	poor	poor
Composites	good	excellent	poor
Plastics	bad	good	fair

To achieve the best material choice, each was evaluated to see if they were satisfactory in each of the critical characteristics. All of the materials except the plastics were able to sustain the maximum stresses inflicted on

the aircraft. Plastics were deemed too brittle. Eliminating plastics, this left metals, woods, and composites as potential choices. The next criterion used to examine these materials was their weight. A chart below compares relative densities for some materials in each class.

Densities of Various Materials (lb/in ³)		
Metals	Woods	Composites
Steel .285	Balsa .0058	Fiberglass .005
Aluminum .100	Spruce .016	Plywood .025
Titanium .162	Douglas Fir .020	
Tin .295	Pine .025	

From inspection of the chart, it is obvious to note that the woods and composites are considerably less in weight than metals. The lightest metal weighs almost 5 times as much as the heaviest wood. Therefore, metals were scrapped. While woods and composites have similar low weight characteristics, their costs are wildly different. Composites are expensive to purchase and their availability is limited compared to the scope of this project. Wood, on the other hand, is relatively cheap to buy and can be readily acquired. Hence, wood is best suited for the airframe construction of the aircraft.

There are numerous types of wood to choose from that satisfy the material selection criteria. The most commonly used in RPV applications are balsa and spruce. Both balsa and spruce satisfy the strength requirements with a modulus of rupture of 7,200 psi and 11,150 psi, respectively. However, balsa has a density half that of spruce and would prove to build a lighter airplane. Also, the cost of balsa was significantly less

than that of spruce, nearly 30% in some instances. Hence, balsa was chosen as the material of construction for the airframe.

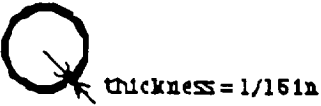
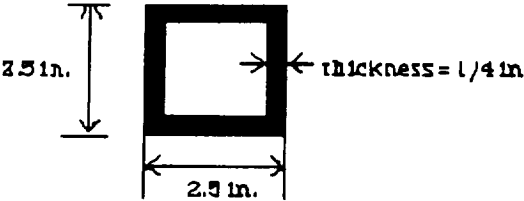

By assuming that balsa was used everywhere for the airplane, another concern materialized. Deflections or bending of aircraft components that could cause instability for the plane while in flight. These deflections reflect the high flexibility characteristics in balsa. Nowhere was this concern illustrated more graphically than at the dowel section of the airplane.

Originally, the design of the dowel section was to be a 1/2 in. diameter solid balsa rod. With this design, the end of the dowel would deflect approximately 2.0 inches under a critical load condition of maximum lift for the horizontal tail section. Intuitively, these deflections would cause undesirable effects on the aircraft. Therefore, an alternate design was necessary to avoid this problem.

Originally, two possibilities were debated as solutions to the problem. One alternative was to have the balsa fuselage section extended to the tail section. The other alternative was to have a graphite tube of 1/16 in thickness as the dowel. The following is a chart comparing the weights and deflections of the alternatives under the critical load condition.

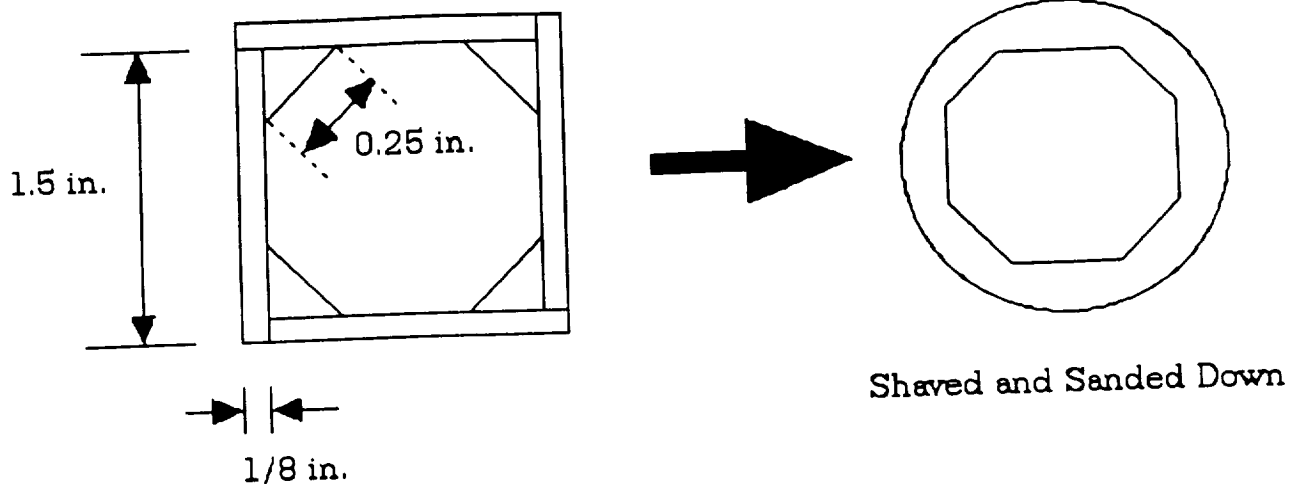
Both designs are similar in weight but the graphite dowel provided better stiffness in avoiding severe tip deflection. Logically, the graphite alternative would provide a better design. However, another problem surfaced. A graphite dowel of the dimension specified could not be located, and if the part was ordered it would take 4 to 6 weeks to arrive. Hence, a time constraint was encountered and another change in design was required; this time to meet availability requirements.

Several "ideas" were bounced around within the design group until someone was wise enough to ask Mr. Joe Mergen for some advice. He

Design Boom Considerations		
Design	Weight	Tip deflection
Graphite Dowel (1/2 in diameter) 	2.13 oz.	0.10 in.
Balsa Box (Extended entire length) 	2.21 oz.	0.50 in.
Balsa Dowel (1/2 in diameter) 	0.20 oz	2.0 in.

recommended constructing a rectangular dowel, from 1/8 in balsa planks, with supports in the corners. Then, he added, one could sand down the edges and corners to produce a cylindrical tube. By choosing this particular design, construction was simple and effective. The following figure depicts the construction.

Final Fuselage Design



The final choice of material selection for the airplane is the skin covering. The skin of the aircraft need only to carry loads in tension, not in compression. A typical choice used by numerous RPV models is mylar "Monokote". Mylar provides excellent strength in tension and creates less skin friction drag.

Weight Estimation

Component Weights and Percentages

One of the considerations to be dealt with first was the total airplane weight estimation. The airplane was determined to have three major contributors to the weight accumulation: aircraft structure, propulsion system, and avionics package. The aircraft structure could not be initially estimated because the size of the biplane had not yet been determined. The avionics package represented difficulties in weight estimation because its contents varied heavily with other design considerations, i.e. to have ailerons or not, to use variable speed control or not, etc. However, the propulsion system, with its three recognizable components: the propeller, the motor, and the battery pack, could be estimated relatively easy. The motor was originally estimated to be 5.0 oz, with a battery pack of 7.6 oz. The propeller weight was originally neglected because of its small contribution to the propulsion system.

Once the weights for the propulsion system were estimated, the actual weight of the airplane was determined. This was accomplished by retrieving weight fractions data on biplanes from RPV and model airplane periodicals. From this data, the propulsion system weight for the aircraft was determined to be 28% of the total weight. Knowing the weight of the propulsion system and its corresponding weight fraction, the total weight of the aircraft was calculated to be 2.8 lbs. The aircraft structural weight was found to be 0.98 lbs. from a 35% weight percentage. The weight fractions and estimated weights for the aircraft are summarized below.

Weight Fractions Estimates		
Component System	Weight Fractions	Component Weight
Structural	35%	15.75 oz.
Propulsion	28%	12.60 oz.
Avionics	37%	16.65 oz.
Total Weight = 45.0 oz.		

Center of Gravity Estimation

To determine the location of the center of gravity for the airplane, accurate values of component weights were required. The weight of each general system was divided into its individual components and the location of each of these components had to be known in order to calculate the center of gravity. The originally established weight estimates had to be refined to more accurately represent the aircraft. These component weight figures are more accurate than the initial weight figures, since the initial figures were based largely on weight percentages and preliminary gross estimates.

In determining the center of gravity, the aircraft was theoretically broken up into two categories: weight components of fixed location and weight components with variable location. The components of fixed location are the structural parts of the aircraft along with the motor and the propeller. The components which can vary slightly in location are the avionics package along with the motor battery pack. Both sets of components, with their weights and locations, determined the center of gravity estimation.

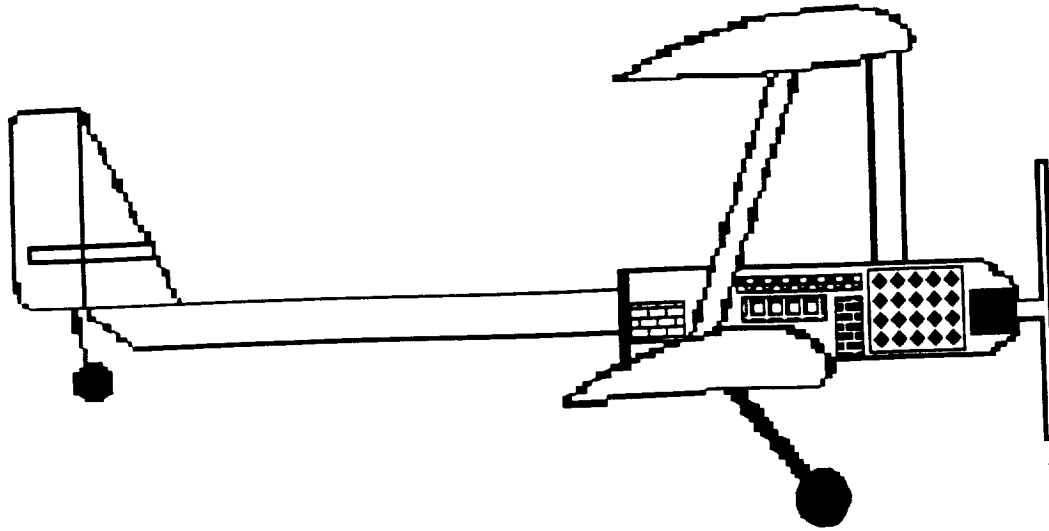
Two tables, one for each weight component category, summarize the RPV's component weights and locations. Also, a schematic is given to illustrate the placement of each of the components in the entire aircraft.

Center of Gravity Locations (Fixed Components)		
Aircraft Component	Center of Gravity	Weight
Propeller	0.0"	0.2 oz.
Engine and mount	0.75"	2.8 oz.
Landing Gear	6.80"	3.0 oz.
Fuselage	7.20"	2.4 oz.
Wings	8.0"	12.0 oz.
Dowel	22.0"	3.0 oz.
Vertical Tail	26.34"	0.5 oz.
Horizontal Tail	27.66"	0.86 oz.
Sub-total Weight =		24.76 oz.

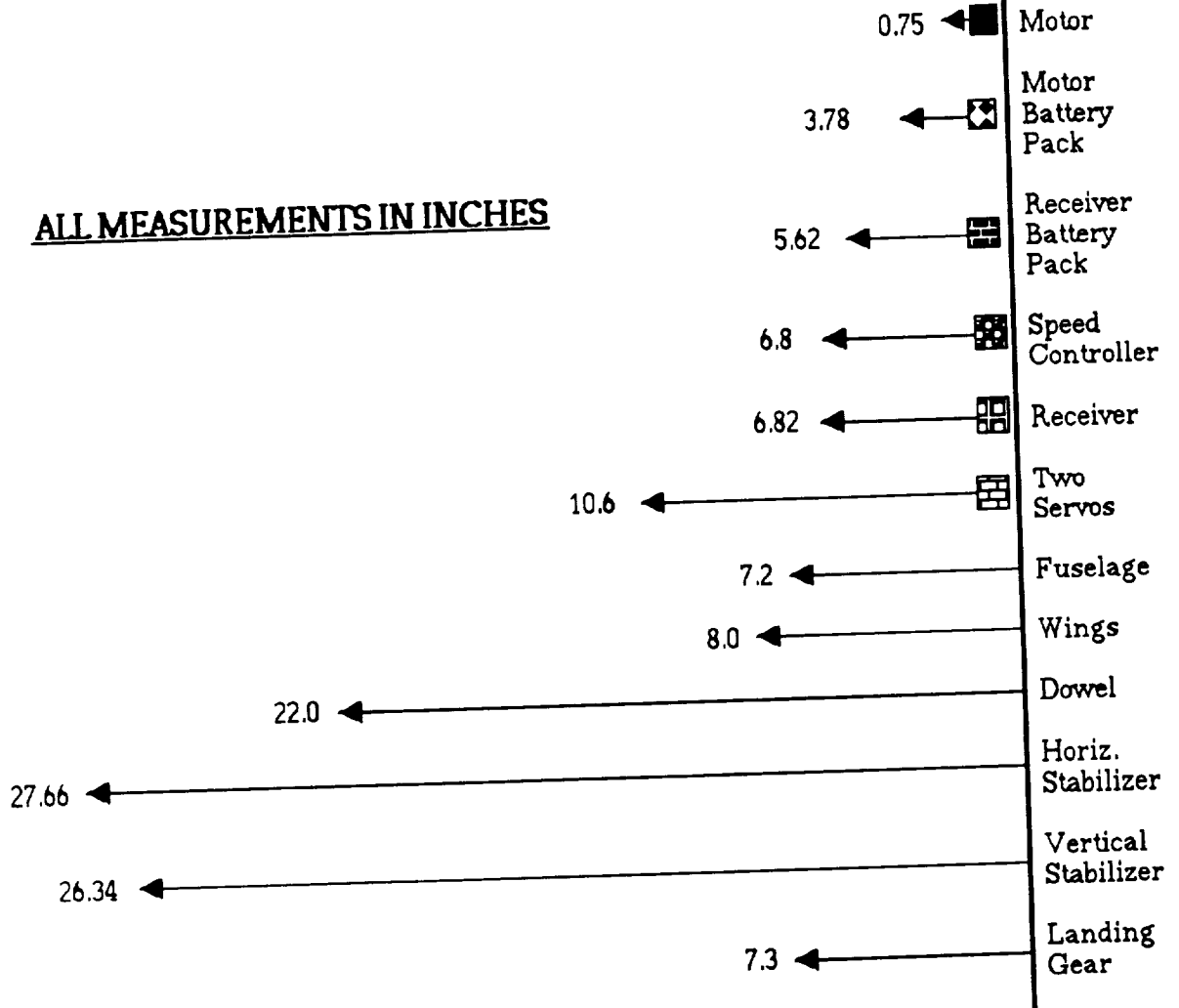
Center of Gravity Locations (Variable Components)		
Aircraft Component	Center of Gravity	Weight
Battery Pack Motor	3.78"	8.0 oz.
Speed Controller	6.80"	2.6 oz.
Receiver	6.82"	1.2 oz.
Receiver Battery Pack	5.62"	2.8 oz.
Two Servos	10.6"	1.2 oz.
Sub-total Weight =		15.8 oz.

The following equation was used to calculate the center of gravity:

$$X_{CG \text{ from nose}} = \frac{\sum X_{CG_{comp}} \times W_{t_{comp}}}{W_{t_{total}}} = \frac{\sum M_{comp}}{W_{t_{total}}} = 7.95 \text{ in.}$$



ALL MEASUREMENTS IN INCHES



The validity of the center of gravity calculation obviously depends on the accuracy of the component weight estimations and their locations. The weight estimations for the propulsion system and avionics package were easily determined and fairly accurate because the actual components had been nearly decided upon. (With the exception of the motor and its batteries) Their locations, on the other hand, are susceptible to change based on decisions in internal layout. For instance, the motor battery pack can move a half inch closer or farther from the motor, and the speed controller's position could be varied an inch forward. The receiver and its battery pack could both be moved approximately 1/4 in. forward; however, the two servos would probably remain in the same location so as to best facilitate their use. These aforementioned changes would have a measurable effect on the center of gravity: 7.15 in. for the internal layout moved as far forward possible, and 7.95 in. for it placed as far aft as possible.

Also, structural component weight estimations were based on guesses of their approximate percentage of the total structure weight. These guesses were based primarily on the size of each component. See figure 14 on next page. If different materials are selected for separate structural components, then their weight estimated would have significant error. For example, a spruce fuselage may be smaller in size to the balsa wing but the fuselage would weigh more.

Structural Components Weight Estimations		
Component	Weight Percentage	Component Weight
Wings	55%	12.0 oz.
Fuselage	11%	2.4 oz.
Dowel	14%	3.0 oz.
Empennage	6%	1.35 oz.
Landing Gear	14%	3.0 oz.

Figure 14

Summary of Aircraft Dimensions

Wings

	<u>Estimation</u>
Wing Area (top)	2.20 ft ²
Wing Area (bottom)	1.65 ft ²
Wing Loading (top)	10.6 oz/ft ²
Wing Loading (bottom)	13.0 oz/ft ²
Wing Span (top)	4.0 ft
Wing Span (bottom)	3.0 ft
Wing Chord	8.0 in. (root) to 5.2 in. (tip)
Wing Planform	taper ratio = 0.65
Wing Location	Biplane (gap & stagger)
Dihedral (top)	2°
Dihedral (bottom)	10°

Horizontal Stabilizer & Elevator

S_s/S_w %	25%
Horizontal Stabilizer Area	0.978 ft ²
Horizontal Stabilizer Chord	0.9 ft
Horizontal Stabilizer Span	1.1 ft
Horizontal Stabilizer Aspect Ratio	1.21
S_e/S_s %	22%
Elevator Chord Length	0.4 ft
Elevator Span Length	1.1 ft
Tail Length (C.G. to Tail A.C.)	17.48 in.
Horizontal Tail Volume Ratio	0.4

Vertical Stabilizer & Rudder

S_v/S_w %	16%
Total Vertical Tail Area	0.633 ft ²
Vertical Tail Volume Ratio	0.19
Vertical Stabilizer Mean Chord	0.52 ft
Vertical Stabilizer Height	1.0 ft
Rudder Chord	0.20 ft
Rudder Height	1.0 ft

Hardware

Motor Size	Silver Streak 035M
Battery Pack	12 Volt, 0.6 amp*hr
Propeller	"Rev-Up" 8-4
Landing Gear	Taildragger
Wheel Material	Plastic, Rubber
Tire Material	Rubber
Main Tire Diameter	1.0 in.
Tail Tire Diameter	0.5 in.
Control Surfaces	Rudder and Elevator
Motor Control	Speed Controller
Elevator and Rudder controls	Servos and Pushrods

Structures List

Main Fuselage Box	1/4 in. balsa sheet
External Struts Mount	1/4 in. balsa sheet
Empennage	3/16 in. balsa plates
Tail Boom	1.5 in. dia. balsa cylinder
Wing Spars	1/4 in. x 1/4 in.
Ribs	1/8 in. balsa sheet
Cap Strips	1/16 in. balsa sheet
Landing Gear Blocks	1/4 in. balsa sheet
Motor Mount	1/8 in. machined Aluminum
Glue	Epoxy and Cyanoacrylate
Wing Skin	Super MonoKote™

Technology Demonstrator

Flight Test Plan

i) Construction

All the avionics and propulsion systems for the aircraft will be permanently mounted within the main fuselage box. The technology demonstrator will be constructed in two main pieces in order to be transported in a 2'x2'x4' box from the University of Notre Dame Aerospace Laboratory to the Loftus Athletic facility. The wings will be one unit and the fuselage and empennage will be compose the other piece. The battery pack may be recharged by removing an access panel located at the top of the main fuselage box.

The only assembly of the technology demonstrator will involve the attachment of the wing structure onto the main fuselage box. The centerline strut will be pegged on a mount at the top of the fuselage. The bottom wing will be strapped on with rubber bands wrapped around the pegs attached to the fuselage. The preparation can be accomplished with only one person.

ii) Taxi Check

Control surfaces should be checked for sticking and binding. This should be an opportunity to check for a properly functioning radio control system. The engine must tested by a taxi at half takeoff speed around the permitted runway area. The taxi run should reveal any loose or unstable parts and problems with steering on the technology demonstrator which can be corrected before the actual takeoff.

iii) **Flight Data Acquisition**

The flight mission (take-off, cruise, and landing) must be carried out as stated in the mission statement. Flight velocity measurements will be made by posting a group member near the flight track (see Figure 15). One member will be positioned at the end of the flight track at position A. This person will mark or estimate the turning radius. Position B and position C will mark the time of the technology demonstrator to pass the positions to obtain flight velocity estimates. Position D and position E will be posted near the pylons to estimate the altitude of the technology demonstrator during the turns (see Figure 15). Another person will be involved in keeping the crowd away from the flight test area. The same person should always be on watch for any sign of danger that would endanger either the group members in the test area or the spectators. Upon landing the technology demonstrator, a visual inspection of the technology demonstrator for any loose or unstable parts and any damaged structural components should be made. The visual inspection should give ample time for repairs before the next flight.

Manufacturing Requirements

Incorporation of the construction of the Stealth Biplane can be done on small capital operation. The Stealth may be built by a small work group consisting of three skilled woodworkers and a field engineer. The group will be involved in a low automation environment. The work group will initially build the components of the Stealth Biplane using conventional sanders and jigsaws. That same work group can also assume accounting, sales, and marketing duties. Assembly procedures will employ unit assembly rather than an assembly line technique. Once sales begin and a profit return

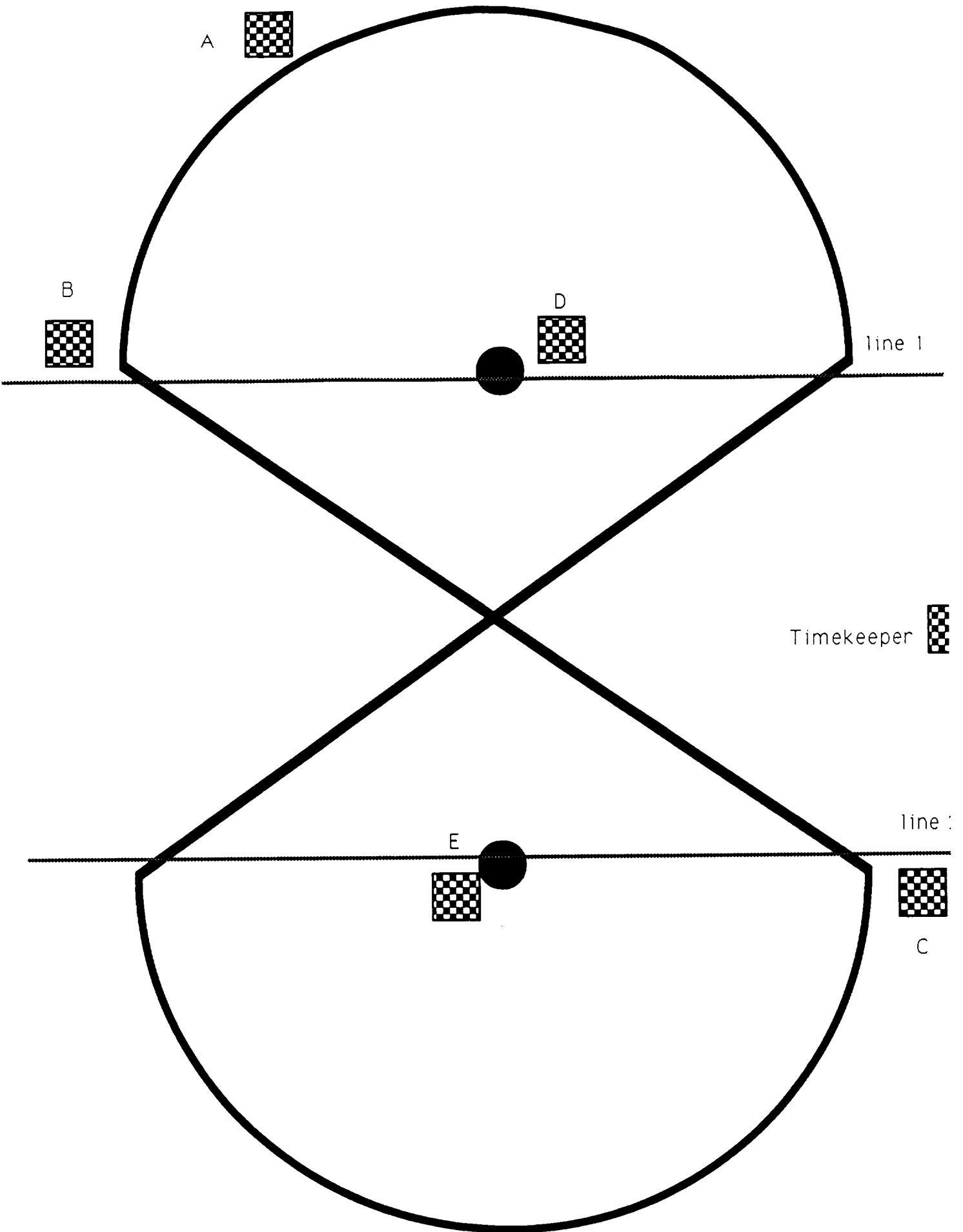


FIGURE 15

begins to show on the bookkeeping, the manufacturing operations can use stamping machines and an assembly line type of operation. The Stealth Biplane may also be sold as a disassembled kit.

Another approach to producing the Stealth Biplane can involve contracting the production of the Stealth to a larger corporation which already has the facilities and resources to produce the aircraft. This leaves the company free to dedicate itself to sales and marketing duties. The company will also be able to expand its sales volume easily without a large capital.

Test Safety Considerations

As with the operation of any vehicle, safety is of prime importance during any time of contact with the Stealth Biplane. If any portion of the biplane is damaged, operation should not take place until appropriate repairs are made. If disaster occurs, the aircraft should be considered the last priority in relation to anything in the immediate vicinity. Three areas of concern - positive control, unplanned descent, and collision avoidance - should be addressed when operating a remotely piloted vehicle . Most of the following is listed in the aforementioned reference.

By outlining and carefully considering those components essential to the control of the RPV, positive control can accurately be assessed and enhanced. Adequate control is more important to safety than the vehicle's structure; therefore, all tradeoffs between these two areas should be treated as such. So as not to produce any signal interruption between the RPV and the ground operator, a transmitting signal well removed from any local radio stations or other transmitting sources is recommended.

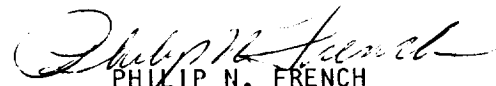
If unplanned descent occurs and landing the vehicle appears necessary, the RPV should be landed in an area devoid of both people and any critical mechanical systems. Should there be any control systems operating obviously, the descent should take place at the slowest possible airspeed to minimize damage both to the RPV and landing area. Also, the motor must be turned off upon impending impact.

Collision avoidance is the last area of system safety to be discussed and is nearly irrelevant in this instance. Avoidance of other aircraft should not be a problem since it is assumed that the flight area will be free of other aircraft. To assure this situation, do not fly more than one aircraft at a time.

Safety is also found in redundancy, such as the use of stronger materials for primary structural supports. Spruce and aluminum may be used at a large expense in weight. Another safety design employed is the usage of ventilation holes at the front and the rear of the main fuselage box. The vented air will provide the cooling necessary for the engine which will be generating large amounts of heat within the main fuselage box. Drag will be a necessary disadvantage to be paid for.

July 24, 1990:

Page 68 removed because of
funding information.


PHILIP N. FRENCH
Document Evaluator

Control Systems

Static Margin and Neutral Point Analysis

The center of gravity of this remotely piloted vehicle, the Stealth Biplane, must be located in front of the stick fixed neutral point location; consequently, the static stability is primarily dependent on the value of the static margin.

The calculation of the static margin was a two step process. The first step was merely a rough calculation as a starting point for the analysis. The second was more involved; therefore, more accurate. The first step of the analysis involved choosing the neutral point and center of gravity based on common values used in RPV production. The neutral point and center of gravity were therefore chosen to be 0.4 and 0.35 times the mean aerodynamic chord, respectively. This yielded a static margin of 0.05 times the mean aerodynamic chord. This corresponds with recommended values for a full-size aircraft⁸. After discussing this value with Dr. Robert C. Nelson, he stated that this is a good target value for an RPV as well.

In the second step of the analysis, the value of $C_{m\alpha}$ for the RPV was set equal to zero to determine a more accurate value of the neutral point. An equation for $C_{m\alpha}$ was derived from first principles since no literature could be found to support a "given" equation. The equation used is as follows:

$$\begin{aligned}
 C_{m\alpha} = & C_{mt} + S_b/S_t C_{mb} - C_{lt}((\alpha_{frl} + i_t)(z_{cg}/c_t + z_t/c_t) + (x_{cgt}/c_t - x_{act}/c_t)) \\
 & - C_{lb} S_b/S_t((\alpha_{frl} + i_b)(z_{cg}/c_t + z_b/c_t) + (x_{cgb}/c_t - x_{acb}/c_t)) \\
 & + C_{lt}(S_t l_t/S_t c_t + S_t/S_t c_t(\alpha_{frl} + i_t - \epsilon)(z_{cg} - z_t))
 \end{aligned}$$

⁸ R. C. Nelson, Flight Stability and Automatic Control, McGraw-Hill, New York, 1989.

where t and b denote the top and bottom wing respectively. All other terminology are consistent with that in Flight Stability and Automatic Control by Dr. Robert C. Nelson.

Although the exact position of the center of gravity could not be known at this point in time, the vertical portion of this parameter is known. Downwash was not included in the calculation because the amount of calculation simplification it provided far outweighed its influence on static margin. Therefore, the neutral point and center of gravity were found to be 9.2 inches and 6.2 inches from the nose of the airplane, respectively. This corresponds to a stick fixed static margin of 7% of the mean aerodynamic chord.

Surface Location and Sizing

The wing spans, chords and tapers were designed first and based on the desired wing loading, 10.2 lb/ft^2 , needed to perform the mission. The top wing will be mounted with 2 degrees of dihedral while the bottom wing will have 5 degrees of dihedral. The distance from the center of gravity to the aerodynamic center of the horizontal tail could be no more than 20 inches and no less than 15 inches. The lower limit was set by the minimum horizontal tail volume ratio and the upper limit was set by the maximum weight of the fuselage section. The lower limit of tail volume ratio for an RPV was found to be 0.7⁹. Therefore, all that was left to be sized was the horizontal and vertical tails. The sizing of the horizontal tail was accomplished in three steps. Initially, reference data was used to validate at rough estimates of the two tail sections. The horizontal tail was initially sized to be 40% the size of the upper wing and the vertical tail 20% the size

⁹ P. F. Dunn, RPV Stability and Control Parameters, 1989.

of the upper wing¹⁰. These values, when placed into the pertinent equations, yielded an angle of attack of the horizontal tail to be negative 4 degrees relative the fuselage reference line. This value was decidedly too negative to be feasibly constructed. A value between -3 and +2 degrees was projected as feasible. Therefore, the second step necessitated the formulation of a simple computer listing used to manipulate these equations more efficiently. After examining the data produced by this simple code, a more appropriate sizing of the tail was arrived at although the angle of attack of the horizontal tail was even more negative. However, at this point downwash had not yet been included and the sections were listed as rectangular planforms.

Obviously, in the third stage of the control system determination, downwash was included and the planforms were shaped to fit more common configurations. This produced a horizontal tail with chord of 4.68 in, span of 7.2 in, area of 34 in², aspect ratio of 1.52 and incidence angle of zero degrees. The elevator was sized to give a $C_{l\delta_e}$ of 0.05 which corresponds to a value common to RPV's¹⁰. The sizing of the vertical tail was much simpler than that of the horizontal tail for two reasons. Firstly, the experience of sizing the horizontal tail helped in avoiding some of the same mistakes; secondly, each reference consulted listed the vertical tail sizings as ratios of the horizontal tail. The same computer listing was used with some pertinent equations changed and the values relevant to the vertical tail are listed:

Area=43 in² Chord=6.6 in Span=7.6 in AR=1.3

The rudder control surface was sized to be 50% of the entire vertical tail (before the leading edge was tapered). This value was taken from Dr. P. F. Dunn's work, RPV Stability and Control Parameters, 1989.

With the tail sufficiently sized, its placement relative to the center of gravity was the last task. As stated earlier, a tail volume ratio no smaller than 0.7 is desired for an RPV. The maximum, taken from the same reference, can be no larger than 1.0. Therefore, after some lengthy calculations, the distance from the center of gravity to the tail's aerodynamic center (l_t) was decided to be 17.5 in. This both agrees with the reference value for tail volume ratio and the (l_t) limits set by feasibility of construction.

During the construction phase of the design, little support existed for the size of the vertical and horizontal tails. Therefore, each was made one and a half times bigger than the original design. This was suggested by the teaching assistants. The vertical stabilizer was also tapered during construction to form a triangular rather than a rectangular planform.

Control Mechanisms

This RPV will use a rudder-wing dihedral combination for roll control, a rudder for yaw control, and an elevator for pitch control. Two servos will be needed to control these surfaces. A third servo is not necessary for throttle control. Therefore, a total of two servos will be used to control the various mechanisms of this RPV. The servos will be located in the main portion of the fuselage above the bottom wing. Control push/pull cables will directly link to the rudder and elevator. The batteries and motor as well as the servos will be accessed from a removable 'door' in the fuselage directly under the top wing.

High Altitude Feasibility

The Stealth Biplane has been designed primarily as a very low altitude flight vehicle. Operating within the confines of an athletic facility at an altitude of only twenty feet allows one to ignore many problems that would arise with outdoor aviation; much less very high altitude operation. Adjusting the aircraft to a high altitude, long duration station keeping mission would open up an entirely new array of engineering problems. The first major design alteration to contend with would be getting the Stealth Biplane to a high altitude operating regime. Either the aircraft would have to remain ground based and circle to the high altitude (approx. 70,000 feet), and in turn requiring a tremendous battery pack, or the Stealth Biplane could be air launched by a conventional flying aircraft at the operating altitude. Ideally, it would be easier to have the RPV dropped from the bay of a transport aircraft, rather than attempt to refit the propulsion system with a larger power pack. Secondly, the RPV will be operating at a much harsher environment. High altitudes typically denote very cold temperatures and unstable air masses. The effects of cold temperatures, though beneficial for propulsion system cooling, could have disastrous effects where structures and materials are concerned. Sub-zero temperatures will cause standard epoxies to crack and become brittle, and structural materials to expand and contract.

Furthermore, the Stealth Biplane has been designed with a maximum load factor of 1.5, whereas the weather effects at these altitudes can cause sudden gusts to easily exceed this load factor, far outside the factor of safety bounds. Thirdly, there does seem to be a definite problem with remotely piloting this vehicle at such high altitudes. A ground based controller would

have no chance of maintaining visual contact with the Stealth and an aircraft based controller would tend to defeat the mission purpose. Thus, an automatic control system would have to be implemented, adding weight and overall difficulty to the design. The only other alternative would be to have an enormous radio receiver on board capable of satellite tracking.

Lastly, at high operating altitudes, the density of the air is drastically less than at sea level. This would impose and even lower operating Reynolds number for the flight. As the Reynolds number drops even further below 100,000, hysteresis effects begin to take place on nearly every airfoil's C_l vs. α curve. This induces sharper wing stalls, with more abrupt loss in lift coefficient, followed by poor stall recovery. Once wing stall occurs in a hysteresis loop, the angle of attack must typically be reduced by 20% to regain normal operation along the $C_{l\alpha}$ curve. Thus, the stall characteristics of the Stealth Biplane would be noticeably poorer at a high altitude regime.

All in all, augmenting the Stealth Biplane would be no simple task. Harsh weather conditions and control problems would inevitably make the RPV larger, heavier, and slower. A thorough study would have to be completed towards such a feasibility in a mission change; but initial estimates make this a difficult project.

Appendix A

RPV Preq Eng Computer Program

PROGRAM RPV;

USES MemTypes,Quickdraw,OSIntf,ToolIntf,PackIntf;

CONST

pi=3.141592654;
density=1.1901; {at 300 meters}
densitye=0.0023801; {at 900 feet}
mu=0.00001789; {kinematic viscosity Ns/m}
mue=0.0000003737; {kinematic viscosity slugs/ft}
grav=9.802; {acceleration of gravity m/s²}
grave=32.2; {acceleration of gravity ft/s²}
sigma=1.0; {density ratio}
fric=0.04; {friction coefficient for}
frice=0.04; {a hard surface/low grass}
e=0.9; {efficiency of aircraft}

VAR

outfile:text; {cricket graph}
UNITS:char; {adaption}
AIR:char;
where:point;
prompt,Origname:Str255;
filename:sfreply;
whocares:OSErr;

Re,chord,TR,Vel,theta,dist,Disttot,GrRollDist,Climbdist:extended;
bank,AR,S,Weight,CL,CD,CDo,Time,RC,gamma,Lift,Drag,AX,BX,ThrustA:extended;
Surf,Area,Power,Timecl,Vst,Vtoreal,b,PR,PA,Vtoideal,btv:extended;
PRX,PRTOP,FT,Q,ThrustR,n,nada,J,CT,CQ,CP,D,rev,PPowerAvail,Torque:extended;

BEGIN

where.h:=190; {cricket graph file save}
where.v:=100;
prompt:='Save RPV Data As:';
origname:='FLY.text';
sfPutFile(where,prompt,origName,NIL,filename);

If (filename.good) then

BEGIN

whocares:=Create(filename.fname,0,'CGRF','TEXT'); {Cricket Graph Format}
Rewrite(outfile,filename.fname);
writeln(outfile,'*');
writeln(outfile,'Re',char(9),'chord',char(9),'Disttot',char(9),
'Vel',char(9),'nada',char(9),'AR',char(9),'Weight',char(9),

```
'CL',char(9),'CD',char(9),'CDo',char(9),'Drag',char(9),
'TR',char(9),'RC',char(9),'Timecl',char(9),'Vtoideal',char(9),
'Vtoreal',char(9),'bank',char(9),'GrRollDist',char(9),
'Climbdist',char(9),'PR',char(9),'PA',char(9),'RC',char(9),
'PPopwerAvail',char(9),'PRX',char(9),'PRTOP',char(9),
'CT',char(9),'CP',char(9),'CQ',char(9),'rev',char(9));
```

```
n:=1.0; {Load Factor}
chord:=0.666667; {Chord length}
TR:=57.0; {Turning Radius}
theta:=11.0; {Climb Out Angle}
ThrustA:=0.5; {Static Thrust Available From Tests}
CDo:=0.04; {Parasite Drag}
S:=3.792; {Surface Area of both wings}
b:=7.0; {Span}
AR:=(b*b)/S; {Aspect Ratio}
Vst:=4.5; {Stalling Velocity}
Vel:=28.0; {Cruise Velocity}
Weight:=2.6; {Aircraft Weight}
rev:=9000.0; {Number of revolutions}
D:=8.0; {Propeller diameter}
```

REPEAT

```
Re:=((density*chord*Vel)/mue);
bank:=((arctan((Vel*Vel)/(grave*TR)))*(180/pi)); {tan theta=V*V/g/r}
dist:=2*(0.75*2.0*pi*TR + 2.0*(SQRT(3600.0-TR*TR))); {distance once}
Disttot:=dist *3.0; {dist 3 times}
Time:=Disttot*Vel;
J:=Vel/(rev*D);
Q:=0.5*density*Vel*Vel; {dynamic pressure}
CL:=(n*Weight)/(Q*S); {lift coefficeint}
Vtoreal:=SQRT(2.0*(Weight/S)/(density*CL)); {real takeoff velocity}
Vtoideal:=(1.20*Vst); {ideal takeoff velocity}
Lift:=(CL*0.5*density*Vel*Vel*S); {lift}
CD:=(CDo+((CL*CL)/(pi*e*AR))); {drag coefficient}
Drag:=(CD*Q*S); {drag}
RC:=((ThrustA-Drag)/Weight); {rate of climb}
PR:=Drag*Vel; {power required}

CP:=0.002498+0.10380*J-0.20446*J*J; {power coefficient}
PA:=CP*density*n*n*n*D*D*D*D; {power available}

CQ:=CP/(2.0*pi); {torque coefficient}
Torque:=CQ*density*n*n*D*D*D*D; {torque}
```

```

CT:=0.030607 + 0.10867*J-0.32963*J*J;           {coefficient of thrust}
ThrustA:=CT*densitye*n*n*D*D*D*D;               {thrust}

nada:=(CT/CP)*J;                                 {propeller efficiency}
PPowerAvail:=PA*nada;                            {shaft power available}

Climbdist:=(20/0.190808);                         {sin11 deg=0.190808}
FT:=(ThrustA-(Drag+mue*(Weight-Lift)));
GrRolldist:=((1.44*Weight*Weight)/(grave*densitye*S*CL*FT));
Timecl:=RC*Climbdist;
PRX:=Vtoreal*Drag;
PRTOP:=Vtoideal*Drag;

writeln(outfile,Re:8:3,char(9),chord:8:3,char(9),Disttot:8:3,char(9),Vel:8:3,char(9),
nada:8:3,char(9),AR:8:3,char(9),Weight:8:3,char(9),CL:8:3,char(9),
CD:8:3,char(9),CDo:8:3,char(9),Drag:8:3,char(9),TR:8:3,char(9),
RC:8:3,char(9),Timecl:8:3,char(9),Vtoideal:8:3,char(9),Vtoreal:8:3,char(9),
bank:8:3,char(9),GrRolldist:8:3,char(9),
Climbdist:8:3,char(9),PR:8:3,char(9),PA:8:3,char(9),RC:8:3,char(9),
PPowerAvail:8:3,char(9),PRX:8:3,char(9),PRTOP:8:3,char(9),
CT:8:3,char(9),CP:8:3,char(9),CQ:8:3,char(9),rev:8:3,char(9));

Vel:=Vel+1.0;
UNTIL (Vel > 40.0);
end;

{ThrustA:=ThrustA+0.01;
UNTIL (ThrustA >4.0)
end;}

{nada:=nada+0.01;
UNTIL (nada >0.7)
end;}

{Weight:=Weight+0.1;
UNTIL (Weight >3.0);
end;}

close(outfile);
readln;
END.

```

Appendix B

KTFTEW Power Available Computer Program

Program KTFTEWProject;

Uses MemTypes, QuickDraw, OSIntf, ToolIntf, PackIntf;

const

pi = 3.141592654;
density = 1.225; {air @ S.L.}
batterycapacity = 6000; {Mah}

Var

outfile:text; {output data file name}
S,W,e,AR,Cdo,range,ia, {Aircraft Parameters}
loadtorque,motoramps,rpm, {Engine Settings for Cruise}
LoadtorqueC,motorampsC,rpmC, {Engine Settings for Climb}
Cl,Cd,D, {flight coefficients}
Powerreq,PowerreqC,Poweravail, {Power Settings for Cruise & Climb}
velocityC,velocity,thrust, {Flight Velocities for Cruise & Climb}
J, {Advance Ratio}
nadaprop, {Propeller Efficiency}
gearrpm, {RPM at gearbox}
Diameter, {Propeller Diameter}
TimetoC, {Time to Climb (sec)}
MahtoC, {Mah used for Climb Phase}
MahLeft, {Mah left for Cruise Phase}
powerin,powerout, {Engine Power Characteristics}
motoreff, {Motor Efficiency}
batteryvolt, {Battery Voltage}
motorohm, {Motor Resistance}
geartorque,geareff,gearpower, {Gear box Characteristics}
batterytime,battdur:extended; {Battery time remaining}

bladetype:char; {Blade Selector}
AIR:char; {Aircraft Selector}
where:point; {don't worry about it, mac stuff}
prompt,OrigName:Str255;
filename:sfreply;
whocares:OSErr;

Begin

where.h:=190;
where.v:=100;

prompt:='Save PROPULSION Data As:';
origname:='Flynn.text';
sfPutFile(where,prompt,origName,NIL,filename);

```

If (filename.good) then
begin
  whocares:=Create(filename.fname,0,'EDIT','TEXT');  (Cricket Graph Format)
  Rewrite(outfile,filename.fname);
  writeln(outfile,'*');
  writeln(outfile,'load torque c',char(9),'load torque', char(9),'velocity c', char(9),
    'velocity',char(9),'rpm c',char(9),'rpm',char(9),'thrust',char(9),'preq
c',char(9),
    'preq',char(9),'pavail',char(9),'time to climb',char(9),' mahtoc',
char(9),'mahleft',char(9),'batterytime',char(9),' range');

  writeln('Enter Aircraft to use A,B,C');
  readln(AIR);

Case (AIR) of
'A': begin
  S:=0.367;
  W:=8.9;
  e:=0.75;
  AR:=12.6;
  Cdo:=0.04;
end;
'B': begin
  S:=0.367;
  W:=8.90;
  e:=0.8;
  AR:=12.6;
  Cdo:=0.04;
end;
'C': begin
  S:=0.367;
  W:=8.9;
  e:=0.85;
  AR:=12.6;
  Cdo:=0.04;
end;
end;

writeln('Enter type of blade for aircraft T,A,Z');
readln(bladetype);

Case (bladetype) of
'T': begin
  J:=(4.0/8.0);
  nadaprop:=-0.38123 + (4.6617*J) - (3.9605*J*J) - (1.7095*J*J*J);

```

```

        Diameter:=8.0*0.0254;

    end;

'A': begin
    J:=(4.0/8.0);
    nadaprop:=0.34903 + (0.88258*J) + (1.7441*J*J) - (3.3338*J*J*J);
    Diameter:=8.0*0.0254;

    end;

'Z': begin
    J:=(4.0/8.0);
    nadaprop:=0.078069 + (2.5764*J) - (2.7452*J*J) + (0.86713*J*J*J);
    Diameter:=8.0*0.0254;

    end;

end;

                                {loop for graphs for aircraft and propellors}
                                {initial values}
                                {semi-close guesses}
motoramps:=1.00;
loadtorque:=0.19;
rpm:=15546.0;

Repeat
    motorampsC:=1.00;
    loadtorqueC:=0.19;
    rpmC:=15546.0;

REPEAT
powerout:=loadtorqueC*rpmC*0.000745;
batteryvolt:=16.2-(motorampsC*0.106);
powerin:=motorampsC*batteryvolt;
motoreff:=powerout/powerin;
motorohm:=0.135*loadtorqueC/motorampsC;
geartorque:=loadtorqueC*2.21*0.95;
gearrpm:=rpmC/2.214;
geareff:=motoreff*0.95;
battdur:=72.0/motorampsC;
gearpower:=powerin*geareff;
velocityC:=gearrpm*J*Diameter/60.0;
Cl:=W/(S*0.5*density*VelocityC*VelocityC);
Cd:=Cdo + Cl*Cl/(pi*e*AR);
D:=Cd*0.5*density*VelocityC*VelocityC*S;
PowerreqC:=D*velocityC;
Poweravail:=gearpower*nadaprop;

TimetoC:=(50.0*W)/(Poweravail-PowerreqC);

```



```
MahtoC:=TimetoC*motorampsC/3.60;
MahLeft:=BatteryCapacity-MahtoC;
```

```
powerout:=loadtorque*rpm*0.000745;
batteryvolt:=16.2-(motoramps*0.106);
powerin:=motoramps*batteryvolt;
motoreff:=powerout/powerin;
motorohm:=0.135*loadtorque/motoramps;
geartorque:=loadtorque*2.21*0.95;
gearrpm:=rpm/2.214;
geareff:=motoreff*0.95;
battdur:=72.0*60.0/motoramps;
gearpower:=powerin*geareff;
velocity:=gearrpm*J*Diameter/60.0;
```

```
Cl:=W/(S*0.5*density*Velocity*Velocity);
Cd:=Cdo + Cl*Cl/(pi*e*AR);
D:=Cd*0.5*density*Velocity*Velocity*S;
Powerreq:=gearpower*nadaprop;
Thrust:= Powerreq/velocity;
Batterytime:=MahLeft*3600.0/(1000.0*motoramps);
Range:=velocity*batterytime;
```

```
writeln(outfile,loadtorqueC:8:6,char(9),loadtorque:8:6,char(9),velocityC:8:6,char(9),
velocity:8:6,char(9),rpmC:8:6,char(9),rpm:8:6,char(9),thrust:8:6,char(9),powerreqC:8:6,
char(9),powerreq:8:6,char(9),poweravail:8:6,char(9),TimetoC:8:6,char(9),
MahtoC:8:6,char(9),Mahleft:8:6,char(9),Batterytime:8:6,char(9),range:8:2);
```

```
rpmC:=rpmC-280.0;
loadtorqueC:=loadtorqueC+1.0824;
motorampsC:=motorampsC+1.500;
```

```
UNTIL (motorampsC >25.00);
```

```
rpm:=rpm-280.0;
loadtorque:=loadtorque+1.0824;    {increment cruise engine settings}
motoramps:=motoramps+1.500;
```

```
UNTIL (motoramps>25.0);
```

```
close(outfile);
end;          { end for IF-THEN check }
readln;
writeln('*');
END.
```

Appendix C

Motor Data Sheet Computer Program


```

If (filename.good) then
begin
  whocares:=Create(filename.fname,0,'EDIT','TEXT'); (Cricket Graph Format)
  Rewrite(outfile,filename.fname);
  writeln(outfile,'*');
  writeln(outfile,'load torque', char(9),'motor amps',char(9),
    'velocity',char(9),'rpm',char(9),'thrust',char(9),
    'preq',char(9),'pavail',char(9));

  writeln('Enter Aircraft to use A,B,C');
  readln(AIR);

  Case (AIR) of
    'A': begin
      S:=0.367;
      W:=8.9;
      e:=0.75;
      AR:=12.6;
      Cdo:=0.04;
    end;
    'B': begin
      S:=0.367;
      W:=8.90;
      e:=0.8;
      AR:=12.6;
      Cdo:=0.04;
    end;
    'C': begin
      S:=0.367;
      W:=8.9;
      e:=0.85;
      AR:=12.6;
      Cdo:=0.04;
    end;
  end;

  writeln('Enter type of blade for aircraft T,A,Z');
  readln(bladetype);

  Case (bladetype) of
    'T': begin
      J:=(4.0/8.0);
      nadaprop:=-0.38123 + (4.6617*J) - (3.9605*J*J) - (1.7095*J*J*J);
      Diameter:=8.0*0.0254;

    end;
  end;

```

```

'A': begin
    J:=(4.0/8.0);
    nadaprop:=0.34903 + (0.88258*J) + (1.7441*J*J) - (3.3338*J*J*J);
    Diameter:=8.0*0.0254;

    end;
'Z': begin
    J:=(4.0/8.0);
    nadaprop:=0.078069 + (2.5764*J) - (2.7452*J*J) + (0.86713*J*J*J);
    Diameter:=8.0*0.0254;

    end;
end;
                                        {loop for graphs for aircraft and propellers}
                                        {initial values}
                                        {semi-close guesses}
motoramps:=1.00;
loadtorque:=1.00;
rpm:=13000.0;

```

Repeat

```

powerout:=loadtorque*rpm*0.000745;
batteryvolt:=16.2-(motoramps*0.106);
powerin:=motoramps*batteryvolt;
motoreff:=powerout/powerin;
motorohm:=0.135*loadtorque/motoramps;
geartorque:=loadtorque*2.21*0.95;
gearrpm:=rpm/2.214;
geareff:=motoreff*0.95;
battdur:=72.0*60.0/motoramps;
gearpower:=powerin*geareff;
velocity:=gearrpm*J*Diameter/60.0;

```

```

Cl:=W/(S*0.5*density*Velocity*Velocity);
Cd:=Cdo + Cl*Cl/(pi*e*AR);
D:=Cd*0.5*density*Velocity*Velocity*S;
Powerreq:=D*velocity;
Poweravail:=gearpower*nadaprop;
Thrust:= Powerreq/velocity;
Range:=velocity*batterytime;

```

```

writeln(outfile,loadtorque:8:6,char(9),motoramps:8:6,char(9),
velocity:8:6,char(9),rpm:8:6,char(9),thrust:8:6,char(9),
powerreq:8:6,char(9),poweravail:8:6,char(9));

```

```
rpm:=rpm-292.0;
loadtorque:=loadtorque+1.0824;
motoramps:=motoramps+1.200;
```

{increment cruise engine settings}

```
Until (motoramps>25.0);
```

{maximum fused amperage of speed controller}

```
close(outfile);
end;
```

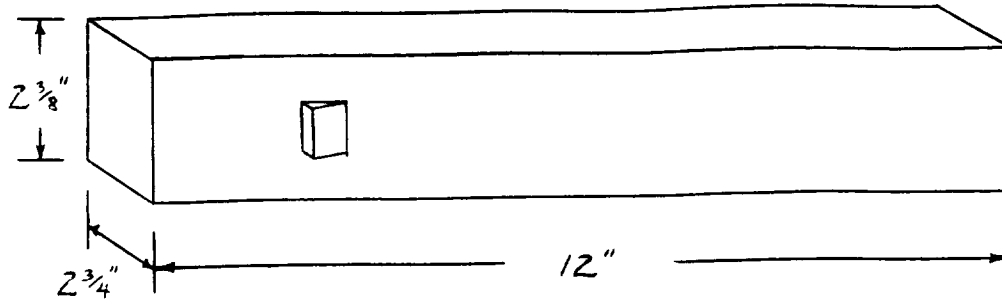
{end for IF-THEN check }

```
readln;
writeln('*');
END.
```

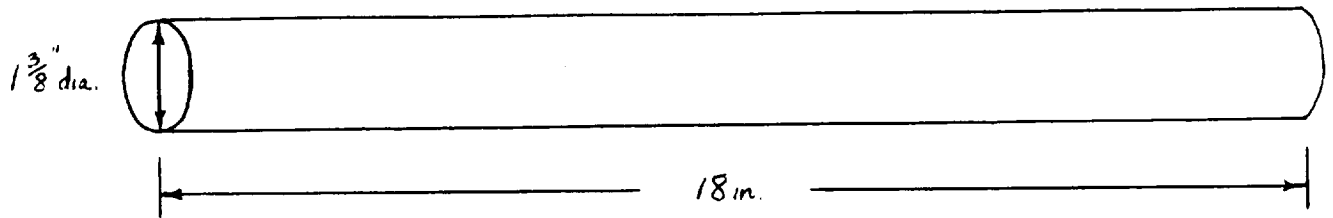
Appendix D

Drag Calculations

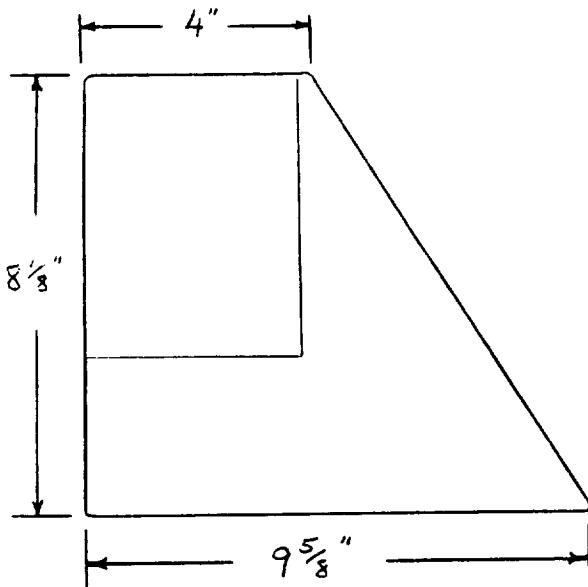
PARTS BREAKDOWN *



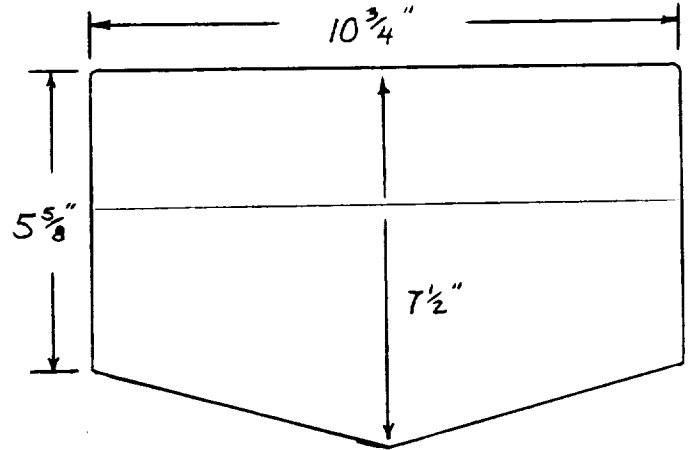
FORE BODY



AFT BODY

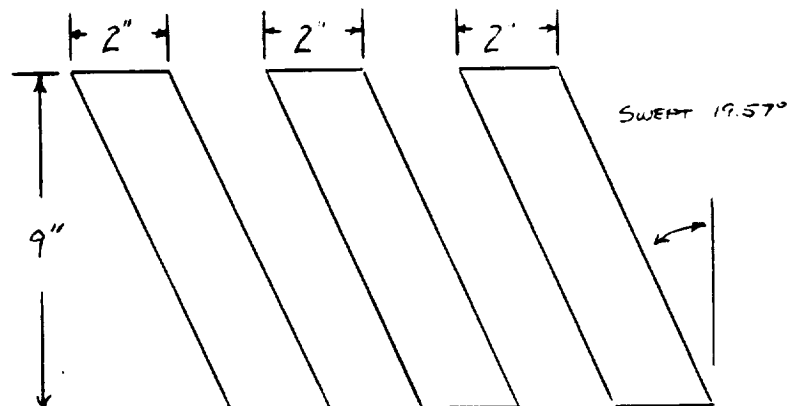


VERTICAL TAIL



HORIZONTAL TAIL

3 WING STRUTS



* DIMENSIONS TAKEN FROM ACTUAL AIRCRAFT AFTER FABRICATION.

Method II Drag Prediction

I. Determination of C_{D0} - body and empennage drag contribution

To begin calculations, the point at which transition from a laminar to a turbulent boundary layer occurs at:

$$x_{\text{trans}} = \frac{\nu \text{Re}}{V} = \frac{(1.653 \times 10^{-4}) (5 \times 10^5)}{(28 \text{ ft/s})} = 2.94 \text{ feet}$$

$$\text{Mach} = \frac{V}{\sqrt{\gamma RT}} = \frac{28 \text{ ft/s}}{\sqrt{(1.4)(1728)(520)}} = 0.0248$$

where the gas constant $R = 1728 \frac{(\text{ft lb})}{(\text{slug } ^\circ\text{R})}$ and temperature $T = 60+460 \text{ } ^\circ\text{R}$

A. Friction Factors

i) fore body

$$\text{Re}_{\text{body}} = \frac{V l_{\text{body}}}{\nu} = \frac{(28 \text{ ft/s}) (1 \text{ ft})}{(1.653 \times 10^{-4})} = 1.694 \times 10^5$$

$$C_{f \text{ laminar}} = \frac{1.328}{\sqrt{\text{Re}_{\text{body}}}} = \frac{1.328}{\sqrt{1.694 \times 10^5}} = 0.003227$$

ii) aft body

$$\text{Re}_{\text{body}} = \frac{V l_{\text{body}}}{\nu} = \frac{(28 \text{ ft/s}) (1.5 \text{ ft})}{(1.653 \times 10^{-4})} = 2.541 \times 10^5$$

$$C_{f \text{ turbulent}} = 0.455 (\log 2.54 \times 10^5)^{-2.58} = 0.0058533$$

iii) horizontal tail

$$\text{Re}_{\text{h tail}} = \frac{V l_{\text{h tail}}}{\nu} = \frac{(28 \text{ ft/s}) (0.547 \text{ ft})}{(1.653 \times 10^{-4})} = 9.264 \times 10^4$$

$$Cf_{\text{ laminar}} = \frac{1.328}{\sqrt{9.264 \times 10^4}} = 0.004363$$

iv) vertical tail

$$Re_{v \text{ tail}} = \frac{V l_{v \text{ tail}}}{\nu} = \frac{(28 \text{ ft/s}) (0.568 \text{ ft})}{(1.653 \times 10^{-4})} = 9.616 \times 10^4$$

$$Cf_{\text{ laminar}} = \frac{1.328}{\sqrt{9.616 \times 10^4}} = 0.004283$$

v) wing struts

$$Re_{\text{ strut}} = \frac{V l_{\text{strut}}}{\nu} = \frac{(28 \text{ ft/s}) (0.167 \text{ ft})}{(1.653 \times 10^{-4})} = 2.823 \times 10^4$$

$$Cf_{\text{ laminar}} = \frac{1.328}{\sqrt{2.823 \times 10^4}} = 0.007904$$

B. Form Factors

Form factors are calculated from the length to diameter ratio for fuselages and from the thickness to chord ratio for wings and control surfaces. For a fuselage the ratio is given by

$$\frac{l}{d} = \frac{l_{\text{ body}}}{\sqrt{\frac{4}{\pi} S_c}}$$

where S_c is the cross sectional area of the fuselage. The form factor is then computed from the equation

$$FF = (1.0 + \frac{60}{\left[\frac{l}{d}\right]^3} + \frac{1}{400} \left[\frac{l}{d}\right])$$

For wings and control surfaces the form factor is given by

$$FF = [1.0 + 0.6\left(\frac{t}{c}\right) + 100\left(\frac{t}{c}\right)^4] [1.34(\text{Mach})^{0.18} (\cos\Lambda)^{0.28}]$$

where Λ is the sweep angle of the maximum thickness line.

i) fore body

$$\left[\frac{1}{d}\right]_{\text{body}} = \frac{1 \text{ ft}}{\sqrt{\frac{4}{\pi}} 0.045 \text{ ft}^2} = 4.161$$

$$\text{FF}_{\text{fore}} = \left[1.0 + \frac{60}{(4.161)^3} + \frac{1}{400} (4.161)\right] = 1.2105$$

ii) aft body

$$\left[\frac{1}{d}\right]_{\text{body}} = 13.091$$

$$\text{FF}_{\text{fore}} = \left[1.0 + \frac{60}{(13.091)^3} + \frac{1}{400} (13.091)\right] = 1.0595$$

iii) horizontal tail

$$\text{FF}_{\text{h tail}} = [1.0 + 0.6(0.01905) + 100(0.01905)^4] [1.34(0.0248)^{0.18}]$$

$$\text{FF}_{\text{h tail}} = 0.6967$$

iv) vertical tail

$$\text{FF}_{\text{v tail}} = [1.0 + 0.6(0.01835) + 100(0.01835)^4] [1.34(0.0248)^{0.18}]$$

$$\text{FF}_{\text{v tail}} = 0.6964$$

v) wing struts

$$\text{FF}_{\text{strut}} = [1.0 + 0.6(0.0625) + 100(0.0625)^4] \times [1.34(0.0248)^{0.18} (\cos 19.57)^{0.28}]$$

$$\text{FF}_{\text{strut}} = 0.7039$$

C. Wetted Area

<u>Aircraft Part</u>	<u>Wetted Surface Area (ft²)</u>
fore body	0.85417
aft body	0.53996
horizontal tail	0.97982
vertical tail	1.53754
wing struts (each)	0.26533

Taking the reference surface area to be the total wing area (3.85 ft²) the parasitic drag of the aircraft excluding the wings is then:

$$C_{D0} = \sum \frac{C_{f\pi} FF_{\pi} S_{wet} \pi}{S_{ref}} = \text{fore body} + \text{aft body} + \text{horiz tail} + \text{vert tail} + 3 \text{ (strut)}$$

$$\boxed{C_{D0} = 0.004851}$$

II. Determination of C_{Dp} and C_{Di} - parasitic and induced drag contribution of wing

The wing parasitic drag coefficient is simply taken from the infinite airfoil data. The coefficient of drag at zero lift is 0.0127.

$$\boxed{C_{Dp} = 0.0127}$$

As stated in the text, the induced drag calculation must be modified for a biplane configuration. Induced drag is given by

$$C_{di} = \frac{S C_l^2}{2b^2\pi e} (1 + \sigma) = \frac{(3.85 \text{ ft}^2) C_l^2}{2(3.5\text{ft})^2(.85)\pi} (1.5) = 0.08827 C_l^2$$

$$\boxed{C_{Di} = 0.088277 C_l^2}$$

III. Total Drag

The total drag polar is then found by adding all the parts: $C_{D0} + C_{Dp} + C_{Di}$.

$$C_D = 0.004851 + 0.0127 + 0.088277 C_l^2$$

$$\boxed{C_D = 0.017552 + 0.088277 C_l^2}$$

Wingbox Structure

